P18 CeraMem Filters for Removal of Particles from Hot Gas Streams

CONTRACT INFORMATION

Contract Number	DE-FG02-90ER80896
Contractor	CeraMem Corporation 12 Clematis Ave. Waltham, MA 02154 (617)-899-0467
Contract Project Manager	Bruce A. Bishop
Principal Investigator	Robert L. Goldsmith
METC Project Manager	Norman Holcombe
Period of Performance	May 19, 1991 - May 19, 1995

OBJECTIVES

The objective of this Phase II SBIR program is the development and demonstration of a novel ceramic filter for particulate removal from hot gas streams resulting from advanced coal conversion processes. This paper describes this novel filter, and provides information on a field testing conducted on a 10 MW pressurized circulating fluidized bed (PCFB) combustor.

BACKGROUND INFORMATION

The need for hot gas cleanup in the power, advanced coal conversion, process and incineration industries is well documented and extensive development is being undertaken to develop and demonstrate suitable filtration technologies. In general, process conditions include (a) oxidizing or reducing atmospheres, (b) temperatures to 1800°F, (c) pressures to 300 psi, and (d) potentially corrosive components in the gas stream. The most developed technologies entail the use of candle or tube filters, which suffer from fragility, lack of oxidation/corrosion resistance, and high cost. The ceramic membrane filter described below offers the potential to eliminate these limitations.

Ceramic Gas Filter Construction

The construction of the CeraMem ceramic filter is based on the use of porous honeycomb ceramic monoliths. These high surface area, low cost materials are widely used as catalyst supports for automotive catalytic converters. The monoliths have a multiplicity of "cells" (passageways) that extend from an inlet end face to an opposing outlet end face. The cell structure can be round, square, or triangular, and the cell "densities" can vary from 25 to 150 cells per

square inch. Porosity of the honeycomb material can be from below 30% to over 50%. The mean pore size can range from about 4 to 50 μm. The superior properties of commercially available honeycomb ceramic monolith materials make them ideally suited for applications requiring high thermal stability, mechanical strength, and corrosion resistance. These rigid ceramics have been used for years as automotive catalyst supports where conditions of high vibration and thermal cycling are encountered in a combustion gas environment. Other applications of these materials as catalyst supports include emission control systems such as catalytic incineration and NOx selective catalytic reduction (SCR).

The monolith structure used for catalyst support material is readily adapted to function as a filter to remove particulate matter from diesel engine exhaust. Unlike the catalytic convertor application in which automotive exhaust flows in a channel flow mode through the honeycomb cells, the diesel particulate filter (DPF) operates as a wall-flow filter. The carbonaceous soot in the exhaust gas is filtered on and within the cell walls of the monolith. This flow path is achieved by modifying the monolith structure by plugging every other cell at the upstream face of the device (Figure 1) with a high-temperature inorganic cement. Cells which are open at the upstream face of the monolith are plugged at the downstream face. Exhaust gas is thereby constrained to flow through the porous cell walls, and at appropriate intervals, the filter is cleaned by burning off the entrapped soot.

A variety of monolith sizes is available for DPF devices. Typical monolith characteristics are a square cell shape, a cell density of 100 cells/in^2, a cell wall side of 0.083 inch, and a cell wall thickness of 0.017 inch. DPF devices operate at least in part as depth filters. The pore size of the cell wall material is quite large (20-35μm), and fine particulates enter and plug the cell wall. Deposition inside the walls leads to pore plugging by particulates and makes regeneration by backpulsing difficult, if not impossible.

Ceramic Filter For Hot Gas Particulate Removal

To filter particulates from hot gas, CeraMem modifies the DPF device described above by applying a ceramic MF membrane to the cell wall surfaces. This technique creates a composite filter which can be operated as a backpulsable surface filter. The thin, membrane coating has a pore size approximately 100-fold finer than that of the monolith support (Figure 2). Thus, the retention efficiency of the filter for fine particles is determined by the membrane pore size. By keeping the membrane coating thin ($\approx$50 μm) the gas flow pressure drop is kept acceptably low. Yet, it is possible to use a large-pored, low-resistance support for the membrane. Because the support is coated by the membrane, the pore size of the support does not affect particle retention and the pore structure of the support does not become plugged by particulate matter.

In operation, particle-laden gas flows into the membrane- coated inlet cells. Particulate matter is collected in the inlet cells and the filtered gas exits the module via the downstream cells. As particulate material accumulates, pressure drop increases to a preselected level at which time the filter is cleaned by online backpulsing from the downstream end of the filter.

The compactness of the filter relative to other gas filters is evident from the data of Table 1. This compactness leads to small filter housings since the filters can be installed in a closely packed array in the vessel. Both the filters and total filter systems are expected to have costs much lower than those of traditional hot gas particulate filtration systems.

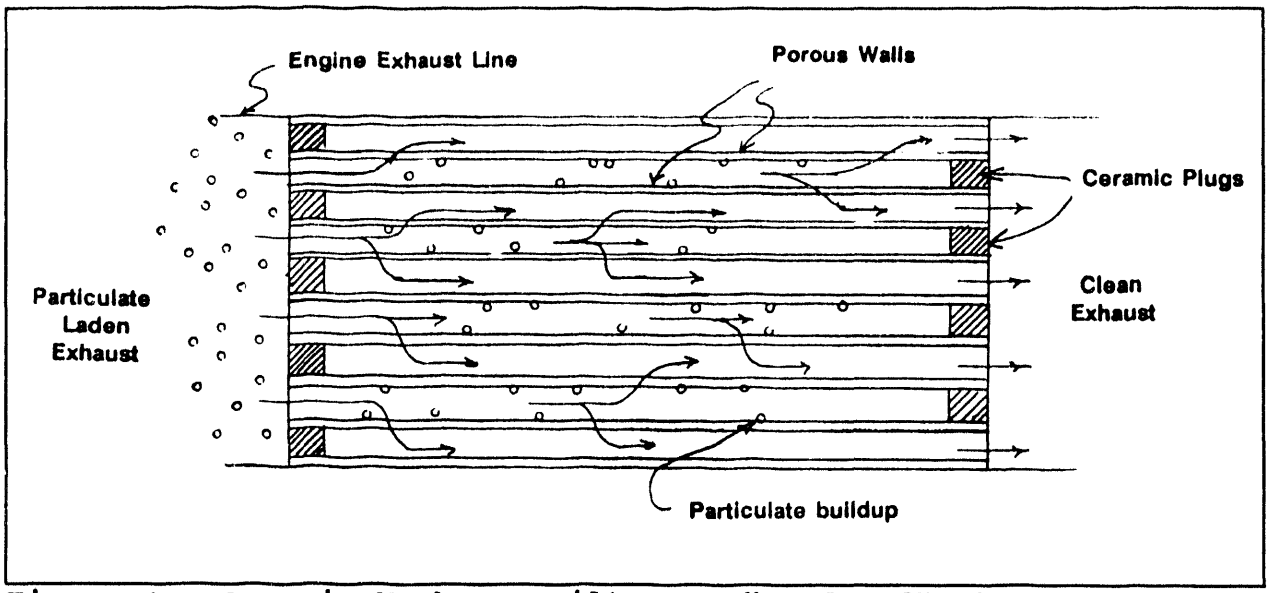

Figure 1. Ceramic Membrane Filter In "Dead-End" Flow Configuration

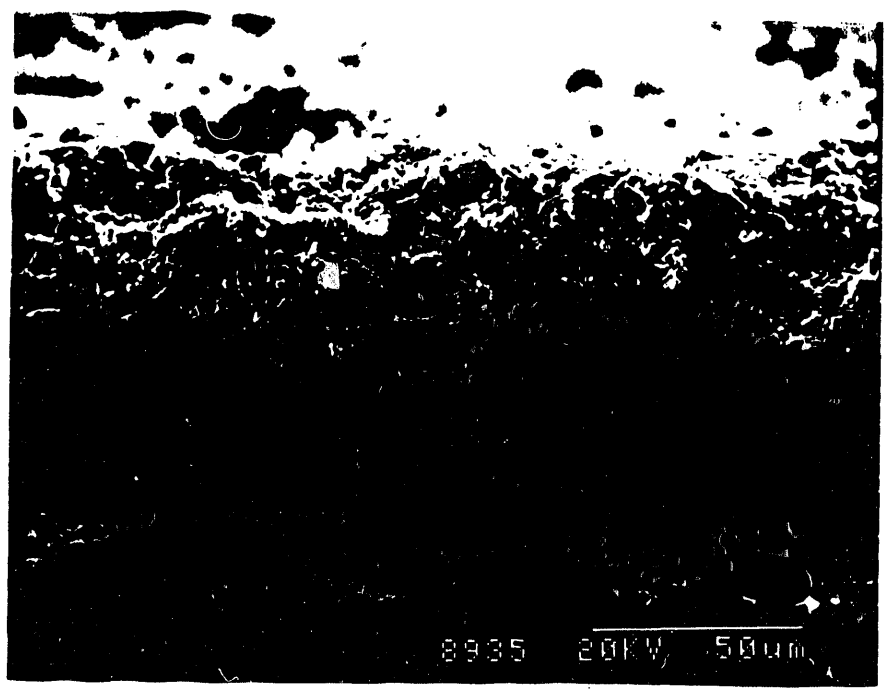

Figure 2. Scanning Electron Micrograph Of Membrane Coating

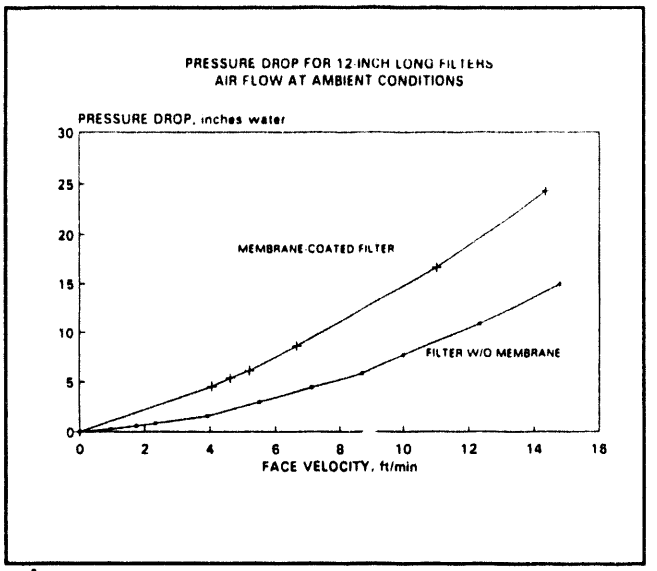

Figure 3. Pressure Drop vs. Flow For Ceramic Membrane Gas Filters

Table 1. Comparison Of Ceramic Membrane Filter With Other Filters

Filter Type	Filter Dimensions	Filter Area (ft^2)	Area/Volume ratio (ft^2/ft^3)
CeraMem	6" sq. x 12" long	37	155
Fabric Bag	6" ϕ x 20' long	31	8.5
Candle	2.5" ϕ x 59" long	2.8	20
Crossflow	11.8" x 11.8" x3.9"	8.3	26.5

Figure 3 shows flow versus pressure drop data for 12" long filters with and without the membrane coating. The membrane coating increases the resistance over that of an uncoated filter about two- to three-fold. For the uncoated filter, the increase in pressure drop with increasing filtration rate is caused by pressure drop in the filter passageways. For membrane coated filters the primary resistance to gas flow is that of the membrane coating itself.

PROJECT DESCRIPTION

The project involves three major tasks:

(1) Ceramic Membrane Filter Development

(2) Filter Demonstration in Field Trials

(3) Full-Size System Design and Costing

The first task has been completed, and the results have been reported in previous project progress reports to the DOE. The focus of this paper will be on task (2).

Filter Demonstration in Field Trials

Field testing of the CeraMem ceramic hot gas filter was conducted at A. Ahlstrom Corporation's 10 MWth PCFB test facility in Karhula, Finland between August 23 and September 8, 1993. During this period, 33 hours of filter operation while exposed to PCFB coal fired conditions were accumulated. The test filters were twelve EX-54 9" diameter x 12" long filters each with 70 square feet of filtration area in the 100 cell per square inch (cpsi) geometry. These filters had the ceramic membrane and cement cell plugs developed for this hot gas application.

Figure 4 shows how Ahlstrom installed and oriented the filters inside their filter pressure vessel. Each filter was wrapped with a ceramic fiber mat and mounted in a 10" ϕ x 13" long casing.

Figure 5 shows a schematic of the Ahlstrom designed backpulse air cleaning system. On-line cleaning of each 4 filter duct in a 1-2-3 sequence was initiated manually or automatically by an adjustable timing device. The pulse air reservoir was maintained between 215 psig and 235 psig

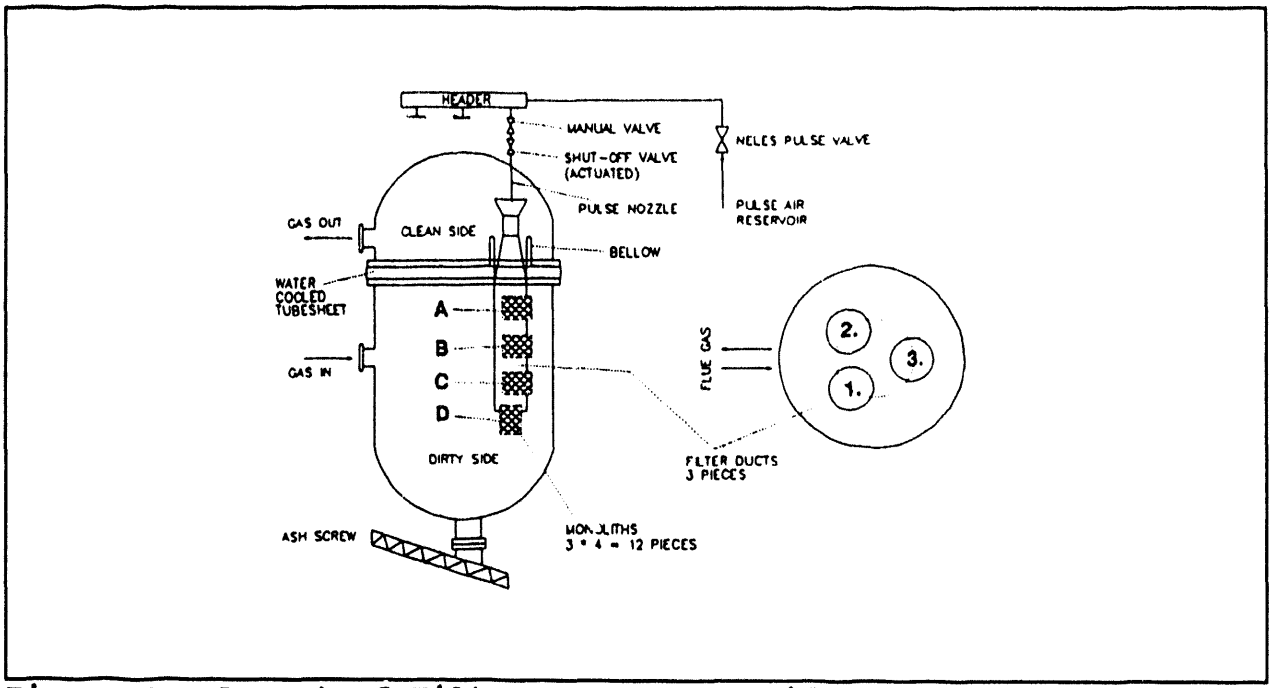

Figure 4. Layout of Filter Elements Inside the Pressure Vessel

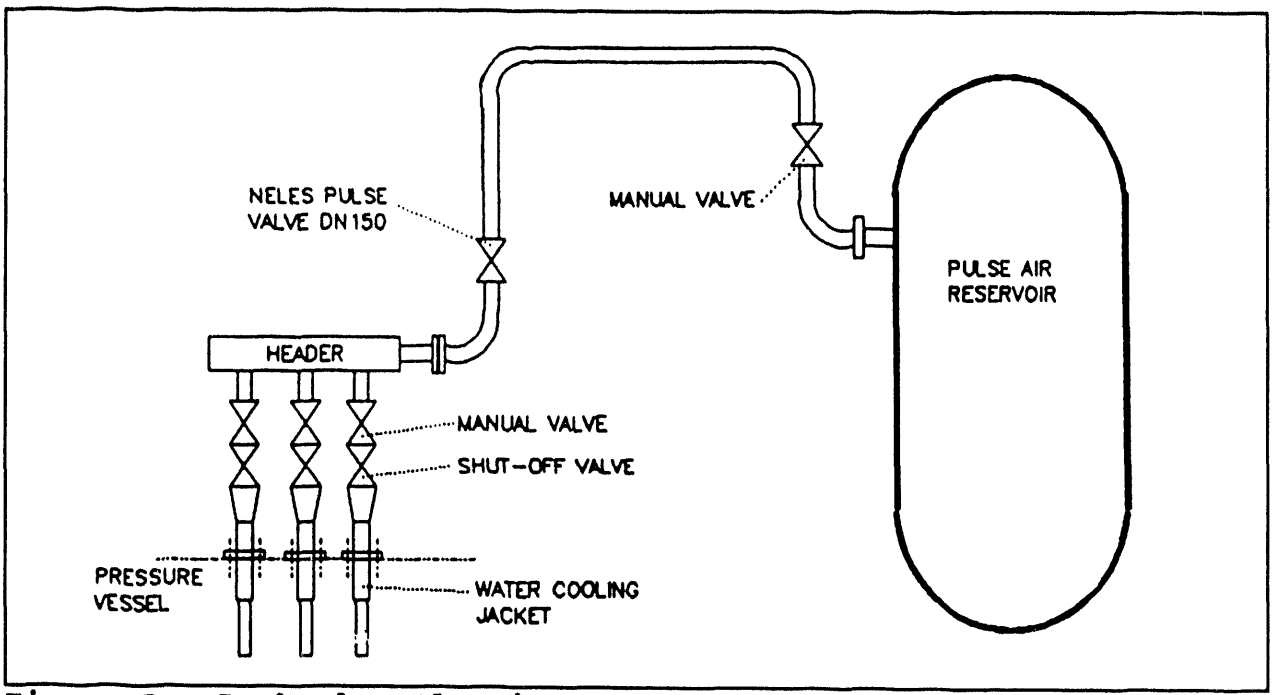

Figure 5. Backpulse Cleaning System

and followed ambient temperature.

RESULTS

Three test runs at coal fired conditions were accomplished before the testing was terminated. Each of these runs was preceded by a PCFB test facility heatup and checkout period using natural gas, light fuel oil and heavy fuel oil prior to conversion to firing with Illinois No. 6 coal and Iowa Industrial Limestone No. 1 in a coal-water slurry. Low dust loads present in the hot gas generated from gas and oil firing generally required manual pulsing to clean the filters and reduce pressure drop during these periods.

a. First Test Run (August 26, 1993) Summary

The first test run on coal generated hot gas lasted about four hours before an ash removal system problem caused a facility shutdown. This initial run achieved an initial baseline and subsequently stable post cleaning pressure drop level of 12" WC. The average operating conditions during the run were 132 psig, 1400°F, and a filter face velocity of 2.24 fpm. Pulse cleaning (at 217 psig) occurred 32 times at 7 minute intervals and maintained peak on-line filtration pressure drops around 32" WC with periodic spikes to between 40" WC and 56" WC in 37% of the cycles. Figure 6 contains the data for this 4 hour run.

b. Second Test Run (September 2-3, 1993) Summary

The longest of the test runs was the second. About 20 hours of operation were achieved at two sets of power level conditions. The PCFB combustor power level was 60% for the first 17 hours of the run, and 80% for the last 3 hours. The 17 hour "A" run average conditions were 129 psig, 1440°F, and 2.30 fpm filter face velocity. During this run, a new baseline and subsequently stable post cleaning pressure drop level of 16" WC was maintained. Pulse cleaning (at 232 psig) occurred 189 times at intervals of 6 minutes and maintained peak on-line filtration pressure drops around 36" WC with periodic peaks to between 40" WC and 60" WC in 15% of the cycles.

The 3 hour "B" run average conditions were 128 psig, 1520°F, and 3.18 fpm filter face velocity. During this run, the baseline shifted to 22" WC due to increased flow rate (face velocity) and higher temperature. Stable post cleaning pressure drop at the new level of 22" WC was again maintained. Pulse cleaning (at 232 psig) occurred 43 times at intervals of 6 minutes and maintained peak on-line filtration pressure drops around 44" with periodic peaks to between 52" WC and 80" WC in 26% of the cycles. Figures 7, 8, and 9 show the data for this 20 hour run.

Failure of the single pulse cleaning valve resulted in an on-line filtration pressure differential excursion of about 100 psi across the filters. The test run ceased and the facility was subsequently shutdown for repair.

c. Third Test Run (September 8, 1993) Summary

Following the pulse valve repair, the filters were pulse cleaned cold about 50 times. Visual inspection revealed substantial (50%) filter cell plugging and some dust evident in the clean gas duct. Following re-start, and in spite of a high filter pressure drop level of 44" WC, a third test run was initiated. This run lasted about 5 hours before being voluntarily shutdown. Upon inspection, the filters were found to be fractured within the holders. This failure was probably caused by the extreme differential pressure (100 psi) imposed across filter elements while being restrained by the holder's retaining ring. Since

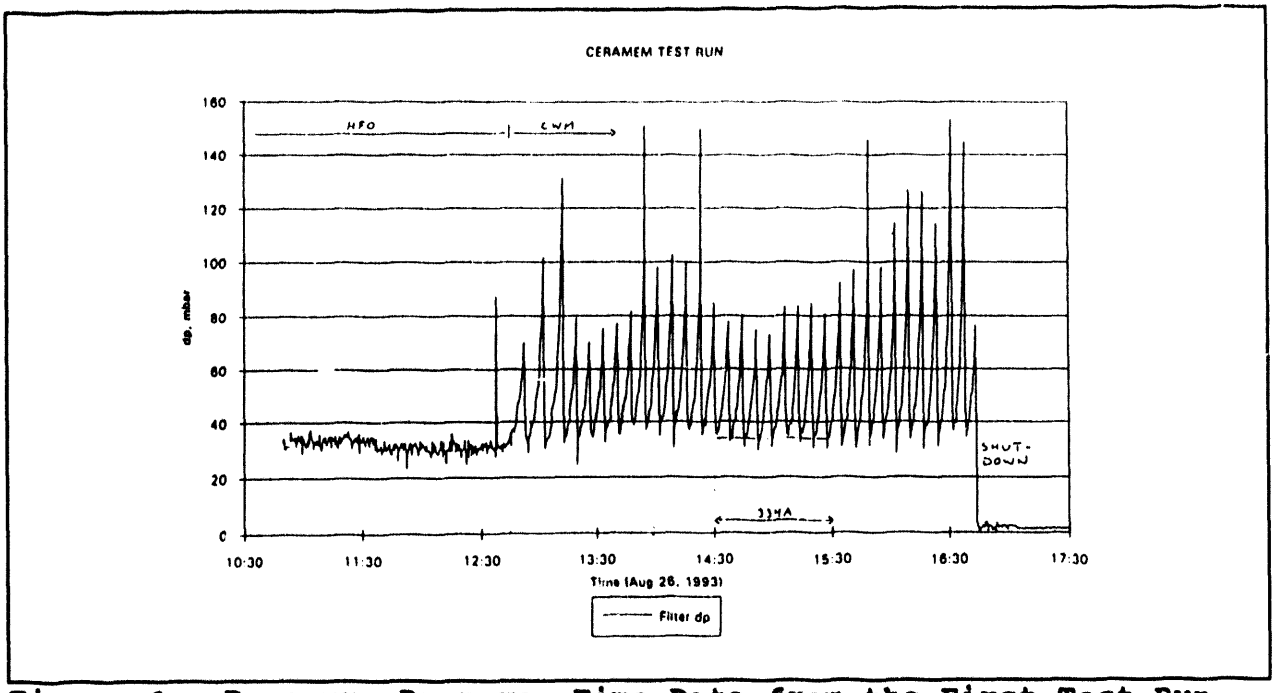

Figure 6. Pressure Drop vs. Time Data from the First Test Run

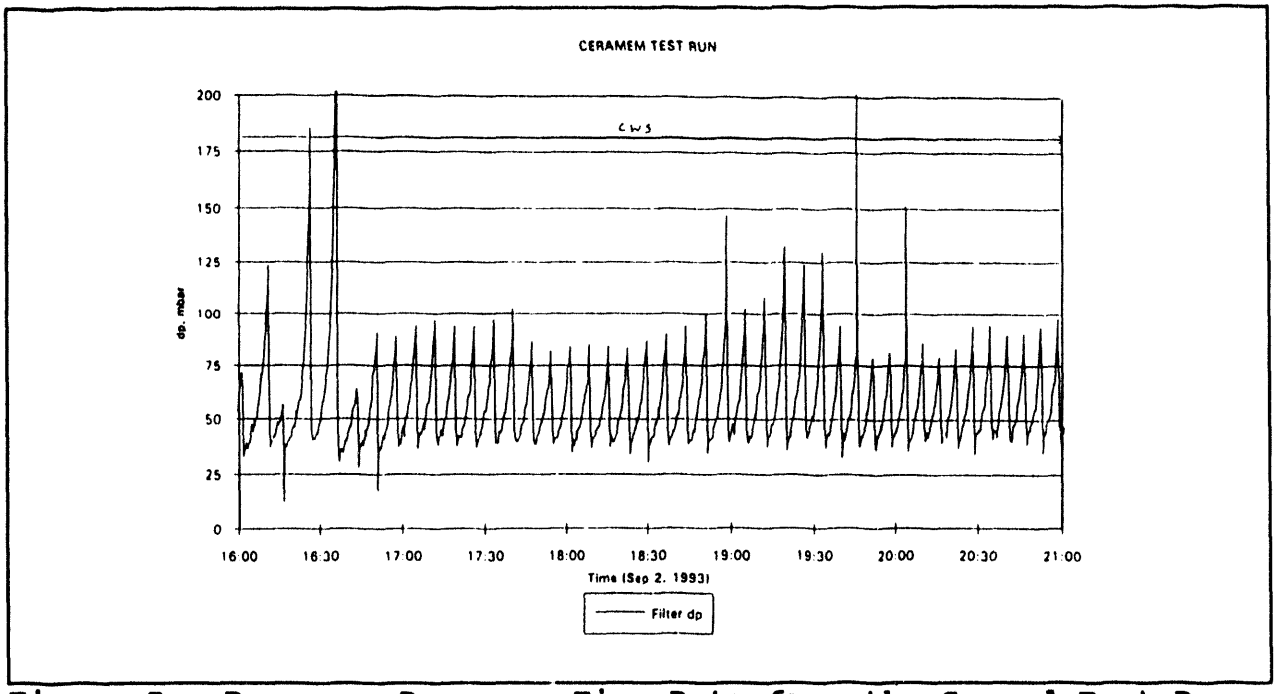

Figure 7. Pressure Drop vs. Time Data from the Second Test Run

AIIM

Association for Information and Image Management

1100 Wayne Avenue, Suite 1100
Silver Spring, Maryland 20910

301/587-8202

Centimeter

Inches

MANUFACTURED TO AIIM STANDARDS
BY APPLIED IMAGE, INC.

6 of 6

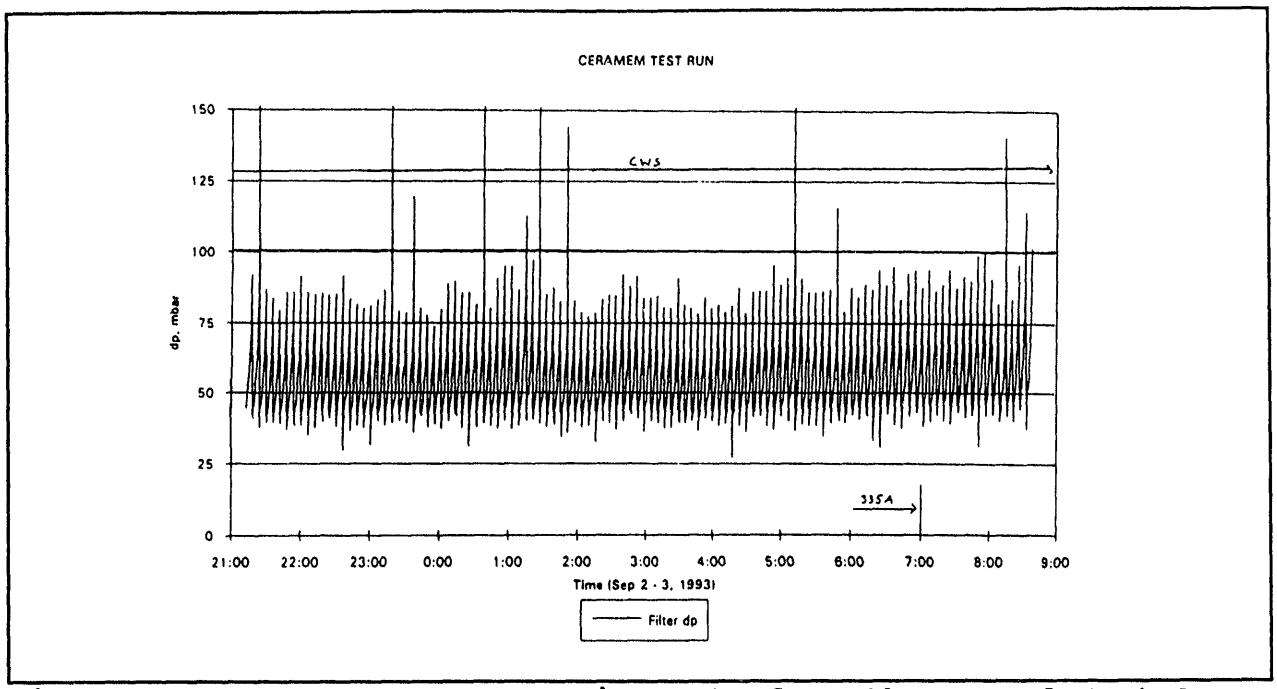

Figure 8. Pressure Drop vs. Time Data from the Second Test Run

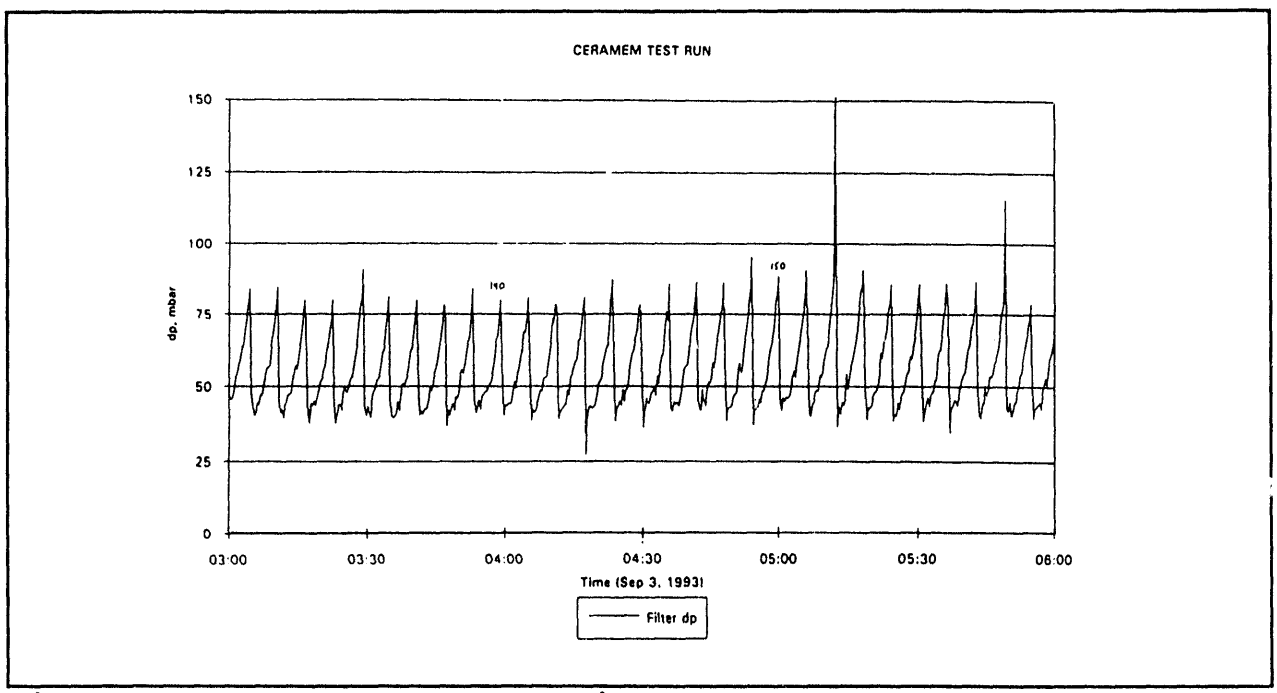

Figure 9. Pressure Drop vs. Time Data from the Second Test Run

the filter boundary had been breached by the fracture and substantial filtration area lost as a result of cell plugging, the data taken during this run was considered invalid and is not included here.

DISCUSSION

Although this test campaign was not of sufficient length to be considered a "demonstration" and fell considerably short of the 6 month objective, certain valuable information was learned from these short term test runs with multiple filters configured in a representative commercial PCFB filter vessel.

Cleanability

Multiple ceramic hot gas filters 9" diameter by 12" long (100 cpsi) were effectively regenerated on-line to initial baseline run pressure drop levels under PCFB conditions over short (up to 20 hours) periods of time. However, on subsequent runs following a previous shutdown, a new higher initial run pressure drop (16" WC from 12" WC) appears to be established while operating at the same conditions. Notwithstanding, the ability to recover back down to that new level was still accomplished. High dust loads (8000 ppmw) in the inlet gas and low volumetric dust holding capacity in the filter resulted in short cleaning cycle times between 4 and 7 minutes.

Clean Filter Pressure Drop

Determination of actual hot clean baseline pressure drop for 12" long 100 cpsi filters at desirable operating face velocities was performed in the early testing. Achieving operation at a level of 12" to 16" WC at 1400°F and 2.5 fpm face velocity was considered acceptable.

Filtration Cycle Behavior

Pressure drop was observed to increase at an accelerating rate during the filtration cycle. This phenomenon is characteristic of the filter's honeycomb goemetry and the filtration mechanism within the filter. A reduction of actual filtration area occurs as the filter cell fills with dust thus increasing actual face velocity (pressure drop); an increase in resistance (pressure drop) occurs through the membrane/wall as dust builds on the surface; and an increase in resistance (pressure drop) occurs to channel flow as the channel narrows with increasing dust buildup on the walls. It should be noted that the cleaning cycle was initiated on a timed basis, resulting in variability and instability of maximum pressure drop level reached before cleaning.

CONCLUSIONS

A novel ceramic membrane filter has been developed and tested for a short period on hot gas stream from a 10 MW PCFB . The filter has the attributes of ultra-high particulate removal efficiency, complete regenerability, compactness and low cost. Continued testing of the filter in hot gas environments, for long duration, and to determine its resistance to attack from potentially corrosive components of the gas streams is underway.

P19 Development of Disposable Sorbents for Chloride Removal from High-Temperature Coal-Derived Gases

CONTRACT INFORMATION

Contract Number DE-AC21-93MC30005

Contractor

SRI International
333 Ravenswood Avenue
Menlo Park, CA 94025
(415) 326-6200

Contract Project Manager Gopala N. Krishnan

Principal Investigators

G. N. Krishnan, B. J. Wood, and A. Canizales (SRI International)
R. Gupta and S. D. Sheluker (Research Triangle Institute)
R. Ayala (GE Corporate Reseach and Developement)

METC Project Manager Ronald K. Staubly

Period of Performance September 30, 1993 to September 29, 1995

Schedule and Milestones

FY94 Program Schedule

Task	S	O	N	D	J	F	M	A	M	J	J	A	S
Submission of NEPA Information													
Sorbent Preparation and Characterization													
Provision of a Bench-Scale Unit													
Bench Scale Testing													
Parametric Testing*													
Data Analysis													

* Scheduled to be initiated in January 1995.

OBJECTIVE

The objective of this program is to develop alkali-based disposable sorbents capable of reducing HCl vapor concentrations to less than 1 ppm in coal gas streams at temperatures in the range 480° to 750°C and pressures in the range 1 to 20 atm. The primary areas of focus of this

program are investigation of different processes for fabricating the sorbents, testing their suitability for different reactor configurations (fixed-, moving-, and fluidized-bed reactors), obtaining kinetic data for commercial reactor design, and updating the economics of the process.

BACKGROUND INFORMATION

Coal is a complex and heterogeneous substance that contains several impurities, including sulfur, chlorine, nitrogen, and metal compounds. The integrated coal gasification combined cycle approach is an efficient process for producing electric power from coal by gasification, followed by high-temperature removal of gaseous impurities, then electricity generation by gas turbines . Alternatively, molten carbonate fuel cells may be used instead of gas turbine generators. In either case, the coal gas must be treated to remove impurities such as hydrogen chloride (HCl), a reactive, corrosive, and toxic gas, which is produced during gasification from chloride species in the coal.

Concentrations of HCl in coal gas have not been determined precisely, but they are estimated to be in the range 1 to 500 ppm (TRW, 1981). Bakker and Perkins (1991) point out that concentrations of HCl in coal gas can be about five times higher than those in coal-fired boiler combustion gas streams because of the lower volume of the coal gas. The actual concentration of HCl vapor in a coal gas stream will depend on the chlorine content of the coal, the gasification temperature, and the type of gasifier. For example, an oxygen-blown gasifier that produces a medium-Btu coal gas will have a higher HCl concentration than an air-blown gasifier that produces a low-Btu fuel gas.

The high-temperature molten carbonate fuel cell (MCFC) is a promising device for future IGCC power generation plants because of its high efficiency. However, for sustained and efficient operation of the MCFC, the feedgas must be free of contaminants such as particulate matter, sulfur, and chloride species. Halogen compounds are deleterious to MCFCs because they can lead to severe corrosion of cathode hardware (Kinoshita et al., 1988). HCl also can react with the molten carbonate electrolyte to form corresponding halides such as LiCl and KCl. The high vapor pressures of these halides increase the loss of electrolyte. The allowable HCl concentration in the feedgas to such a fuel cell is estimated to be less than 1 ppm (Gillis, 1980).

The role of HCl as an impurity in coal gas used to fuel a gas turbine is not well defined and currently no concentration limit standards exist. In spite of the absence of specified limits, the removal of HCl vapor from the fuel can only be beneficial for IGCC systems, because the presence of HCl vapor is generally deleterious to the metal components of the IGCC systems. Perkins et al. (1990) report that the chloride deposits found on syngas coolers accelerate the corrosion of the heat exchanger material. HCl reacts with the deposited slags forming low-melting iron chlorides, and thereby accelerates the corrosion rate.

A number of processes are available for removing HCl vapor from industrial and incinerator waste gases. These processes scavenge HCl by adsorption onto activated carbon or alumina or by reaction with alkali or alkaline earth carbonates or oxides. In chemical plants where HCl must be removed from process feedstocks, commercial sorbents called chloride guards are marketed by catalyst manufacturers and these sorbents are relatively expensive. These sorbents reduce chloride contaminant levels to <l ppm, but they must operate at temperatures <450°C. Furthermore, none of them are economically regenerable. Hence, inexpensive and disposable sorbents are needed for the chloride removal in hot coal-derived gas streams.

Equilibrium thermodynamic calculations provide a theoretical limit to which chloride vapor level can be reduced by using sorbents. We calculated the equilibrium levels of both HCl and metal chloride vapor level as a function of temperature for various alkali and alkaline earth chlorides. Of the alkali salts considered, potassium yielded the lowest HCl vapor levels. However, at temperatures above 1000 K, NaCl(g) has a lower vapor pressure than KCl(g) (Table 1). In addition, the sodium minerals are more abundant than potassium minerals. Of the alkaline earth compounds considered, only barium compounds have both low equilibrium HCl level and chloride vapor pressure. But, the HCl vapor level in equilibrium with $BaCl_2$ exceeds that in equilibrium with NaCl.

Table 1. Equilibrium Vapor Pressures over Alkali and Alkaline Earth Chlorides

	Equilibrium Pressure (10^{-6}atm)	
System	HCl(g)	MCl(g)
800 K		
Na	0.5	<0.01
K	0.05	0.25
Ba	8.0	<0.01
Ca	560.0	<0.1
Sr	79.0	<0.01
1000 K		
Na	4.0	62.0
K	0.4	120.0
Ba	54.0	<0.1
Ca	1400.0	<0.1
Sr	260.0	<0.1

Previous bench-scale studies have shown that disposable sodium-based sorbents have sufficient chemical reactivity to reduce HCl vapor in simulated coal gas streams in the temperature range from 540° to 650°C. Early experimental studies at Physical Sciences, Inc. (PSI) focussed on shortite ($Na_2CO_3 \cdot 2CaCO_3$) and trona ($Na_2CO_3 \cdot NaHCO_3 \cdot 2H_2O$) as candidate sorbents (Ham et al., 1984). Trona exhibited a lower reactivity than shortite, a characteristic that was attributed to sintering of the mineral at the sorption temperature. Battelle Pacific Northwest Laboratories conducted both laboratory- and bench-scale studies to determine the feasibility of simultaneously removing H_2S and HCl in hot coal gas systems by using solid supported molten salts (Lyke, 1985). Using lithium, potassium, and calcium carbonates supported on lithium aluminate, they found that HCl vapor was reduced from about 200 ppm to less than 10 ppm at 800°C and 15 atm. The residual chloride in the gaseous effluent consisted mainly of alkali chloride vapor whose concentration increased with temperature. An operating cost of about $0.008/kWh was projected in a preliminary economic analysis.

Laboratory- and bench-scale experiments were performed by SRI International (Krishnan et al., 1986) to evaluate three natural carbonate minerals—nahcolite ($NaHCO_3$), shortite, and dawsonite ($NaAl(OH)_2CO_3$)—as HCl scavengers for simulated coal gas. A chloride guard (Katalco 59-3) and a commercial flue gas cleanup sorbent (NOXSO) were also examined in the project. All the tested sorbents reacted rapidly with HCl vapor and reduced the HCl vapor concentration from about 300 ppmv to about 1 ppmv. The performance of nahcolite was superior in its adsorption capacity; the spent sorbent contained up to 54 wt% chloride. Furthermore, the presence of H_2S and trace metal impurities in the coal gas did not significantly affect the performance of the bed for HCl sorption. An economic evaluation for HCl cleanup costs in a 100 MW_e plant indicated that the use of nahcolite to remove HCl vapor would add only about $0.002/kWh (2 mills/kWh) to the cost of the generated electric power.

Thus, alkali-based naturally occurring minerals and synthetic sorbents have been shown in bench-scale experiments to be capable of reducing HCl vapor levels to about 1 ppm in simulated coal gas streams.

PROJECT DESCRIPTION

The primary areas of focus in the current program are to investigate different processes for fabricating sorbents suitable for HCl vapor removal in hot, coal-derived fuel gas streams, test their suitability for different reactor configurations (fixed-, moving-, and fluidized-bed reactors), obtaining kinetic data for commercial reactor design, and update the economics of the process. This project is a colloborative effort between SRI, the prime contractor, and subcontractors Research Triangle Institute (RTI) and General Electric Coporate Research and Development (GE-CRD). RTI is developing and testing sorbents for fluidized-bed reactors, while GE-CRDC is preparing sorbents for moving-bed reactors. SRI is preparing and testing sorbents for fixed-bed reactors. The moving-bed sorbents prepared by GE-CRD will be also tested at SRI.

The program is divided into the following six tasks:

1. Information required for National Environmental Policy Act (NEPA)
2. Sorbent preparation and characterization
3. Provision of bench-scale test unit

4. Bench-scale testing
5. Parametric testing
6. Data analysis.

At the beginning of the project, information was provided to the U.S. Department of Energy (DOE) for a NEPA review. The review was completed and authorization was recieved to proceed with the program. Based on earlier studies, nahcolite, an abundant and available natural mineral, was the primary choice for the sorbent material. About 300 kg of nahcolite powder, obtained by solution mining from deposits near Rifle, Colorado, was supplied free-of-charge by NaTec Resources, Inc., Houston, Texas. For testing purposes, the powder was pelletized or granulated with binders and texturizing agents using pilot-scale equipment.

The HCl reactivity and chloride capacity of the granules and pellets are being determined using thermogravimetry and bench-scale reactors both at SRI and RTI using similar equipment. The reactors are typically 5-cm ID and 90-cm long and heated externally using electrical furnaces. Simulated gas mixtures representative of either Texaco oxygen-blown gasifier or METC's GPIF air-blown gasifier are blended using individual gases or binary gas mixtures. A higher than normal level of HCl vapor is used in these tests to reduce the reaction time. The HCl vapor in the product gas leaving the reactor is dissolved in water and the accumulated chloride in the solution is measured with an automated ion chromatograph. The concentration of HCl vapor in the gas stream is calculated by differentiating the cumulative chloride level with respect to time. The analytical system is capable of measuring sub-ppm levels of HCl vapor.

RESULTS

Sorbent samples for testing were prepared by pelletizing or granulating the powder with binders and texturizing agents. Pellets suitable for use in a fixed-bed reactor were extruded in sizes varying from 1.5 to 5 mm. They contained either bentonite (10wt%) or sodium silicate (2 and 5 wt%) as the binder (Table 2). In some cases, methyl cellulose was added as a texturizing agent. The pellets were calcined in air, and during calcination, when the temperature exceeded 150°C, the nahcolite mineral decomposed into sodium carbonate, releasing CO_2 and H_2O:

$$2NaHCO_3\ (s) = Na_2CO_3\ (s) + CO_2\ (g) + H_2O\ (g)$$

The evolution of these gases produced a porous sorbent, but at higher calcination temperatures, the surface area decreased due to sintering of the solid (Figure 1). However, neither the binder composition nor the presence of carboxy methyl cellulose affected the pellet surface area when they were calcined at temperatures higher than 400°C.

The physical properties of two types of pellets were comparable both after calcination and reaction with HCl (Table 3). The crush strengths of the extrudates, as determined by the ASTM method D4179, were similar for all pellets, irrespective of additive. The average crush strength of the pellets calcined at 300°C for 16 h was 450±70 kg/m and that of pellets calcined at 550°C was 700±100 kg/m.

Fixed-Bed Reactor Experiments

The reactivities of different pellet formulations were determined in a thin, fixed-bed reactor operating under near differential conditions. In these experiments, about 2 g of each sorbent was placed in a compartmented tray situated inside a quartz reactor. At 550°C, a simulated gas stream representative of Texaco oxygen-blown gasifier product containing 2000 ppm HCl was passed through the reactor at a rate of 5 SLM. The analysis of the chloride content of the pellets after exposure for 0.5, 8, 24, and 32 h (Table 4) indicated that the pellets made with 5 wt% sodium silicate binder (L-10) had the highest capacity for HCl uptake. The observed fractional chloride content of 0.61 corresponds to nearly 100% conversion of the sodium compounds in the pellets to NaCl. Decreasing the sodium silicate content from 5 to 2 wt% did not change the reactivity initially, but the ultimate chloride capacity decreased. No significant change in the HCl reactivity was observed between the pellets prepared with bentonite as a binder.

Table 2. Sorbent Preparation Paramters of Nahcolite Pellets

Pellet	Fabrication Date	Binder	Size of pellets
L-07	February 94	10% Bentonite+ methocel	3 mm extrudate
L-08	February 94	10% bentonite + methocel	1.5 mm extrudate
L-11	February 94	10% bentonite	3 mm extrudate
L-09	February 94	2% Sodium silicate + methocel	3 mm extrudate
L-10	February 94	5% Sodium silicate + methocel	3 mm extrudate
S-01	November 85	10% bentonite	4 mm extrudate

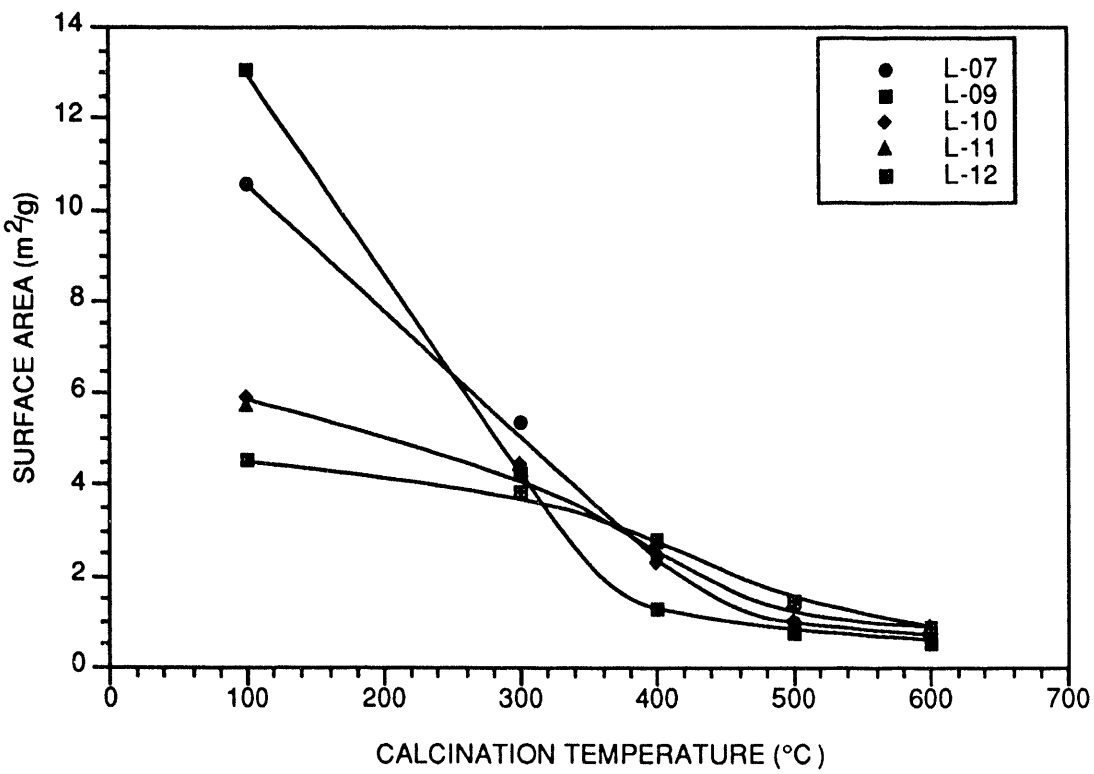

Figure 1. The Change in Surface Areas of Nahcolite Pellets as a Function of Calcination Temperature

Table 3. Physical Properties of Pelletized Sorbents

Parameter	L-10 Calcined	L-10 Spent*	L-07 Calcined	L-07 Spent*
Surface area (m^2/g)	1.0	0.4	1.0	1.8
Bulk density (g/cm^3)	1.1	1.3	1.0	1.2
Pore volume (cm^3/g)	0.29	0.30	0.52	0.27
Average Pore Dia. (μm)	1.0	0.24	0.56	0.36
Porosity (%)	54.9	38.2	54.0	33.4

* Exposed to 1500 ppm HCl at 550°C for 24 h.

Table 4. Chloride Uptake by Nahcolite Pellets as a Function of Exposure to 1500 ppm HCl Vapor at 550°C

	Chloride Content (wt% of the Pellets)				
Time (h)	L-07	L-08	L-11	L-09	L-10
0.5	1.40	1.10	0.00	1.00	0.92
8	15.00	12.00	14.00	22.00	23.00
24	29.00	17.00	39.00	29.00	44.00
32	32.00	40.00	34.00	37.00	61.00

Similar experiments were also carried out at a bed temperature of 450°C (Table 5). At this temperature, the pellets prepared with 5 wt% sodium silicate binder (L-10) had the highest chloride capacity followed by the pellets containing 10 wt% bentonite binder (L-07) with methocel added during preparation. However, the variations in reactivity and chloride capacity between the tested pellets were minor.

The crush strength of the nahcolite pellets did not change significantly after chloride uptake. The initial pellets had a strength of 661 kg/m. After exposure at 550°C for 36 h to an HCl containing gas stream in a deep bed, the pellets which had a chloride content of 25 wt% had a crush strength of 1475 kg/m and those that had 1 wt% had a strength of 830 kg/m. Thus, chloride uptake does not degrade the mechanical strength of the pellets.

Table 5. Chloride Uptake by Nahcolite Pellets as a Function of Exposure to 1500 ppm HCl Vapor at 450°C

	Chloride Content (wt% of the Pellets)				
Time (h)	L-07	S-01	L-11	L-09	L-10
1	1.48	0.30	4.39	5.31	1.79
8	5.90	8.24	9.92	10.1	7.60
24	18.9	–	32.5	26.9	37.0
32	51.1	46.4	45.6	44.8	63.6

Integral, fixed-bed reactor experiments were also conducted with L-10 pellets at 500°C. A deep bed of sorbent pellets (5-cm diameter by 15-cm long) was exposed to a simulated coal gas stream containing 1750 ppm of HCl at a space velocity of 3500 h^{-1}. The HCl level in the reactor exit remained at less than 1 ppm for a period of a 8 h (Figure 2). It required about 11 h to reach the breakthrough level of 10 ppm. When the HCl concentration reached 30 ppm, the experiment was stopped and the spent sorbent was removed from the bed in successive layers (about 1 cm deep) that were analyzed for chloride. The results (Figure 3) showed that the upstream end of the bed was nearly saturated with the chloride whereas the downstream end contained less than 2 wt%. A preliminary analysis of the data using a model for first-order reaction in an integral reactor, resulted in a rate constant of 4 ± 1 mole $HCl \cdot g^{-1}$ sorbent$\cdot h^{-1}$, a value similar to the one obtained in an earlier program at SRI (Krishnan et al., 1986).

Fluidized-Bed Reactor Experiments

Fluidized-bed, bench-scale reactor (2.6-cm ID) experiments were conducted at Research Triangle Institute with nahcolite powder and granules. Nahcolite powder (N-01) in the size range 90 to 300 μm was tested at 550°C in a simulated gas stream representative of Texaco oxygen-blown gasifier product containing 1750 ppm HCl. Experiments were also conducted with a nahcolite sorbent (N-23) granulated (90 to 300 μm in size) with 10 wt% bentonite as a binder. The physical properties of the fresh, calcined, and spent sorbents are shown in Tables 6 and 7.

These experiments also show that the granulated and powder sorbents can reduce the level of HCl vapor in hot coal gas to less than 1 ppm (Figure 4). The HCl breakthrough time at 1 ppm level was about 30 minutes at a space velocity of 4500 h^{-1} ($U/U_{mf} = 5$), but dramatically increased to 720 minutes when the space velocity was decreased to 3000 h^{-1} ($U/U_{mf} = 3.2$). It is believed that at the higher space velocity, the contact between the gas and the sorbent was poor due to the slugging of the bed. Because elutriation of granulated sorbent particles (N-23) occurred at a space velocity of 4500 h^{-1}, experiments were conducted only at a space velocity of 3000 h^{-1}. The granulated sorbent at the decreased gas flow rate was very effective and the 1-ppm breakthrough time was nearly 33 h. The chloride capacity of the granulated sorbent at 10-ppm breakthrough level was 27 wt% whereas only half that value was observed with the non-granulated sorbent (Table 8).

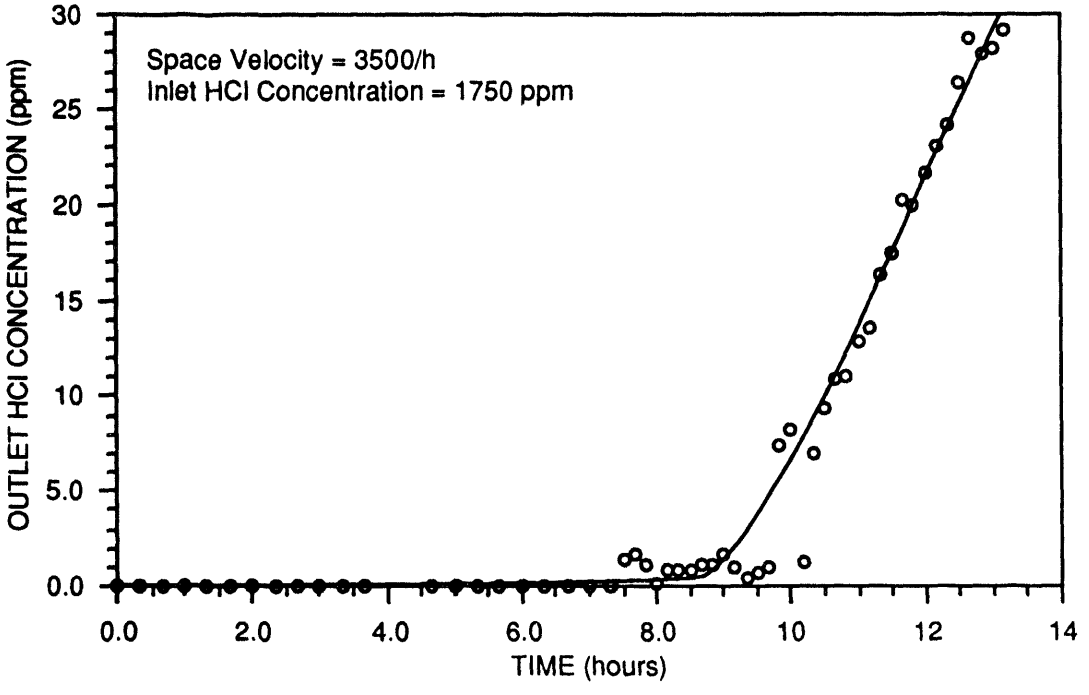

Figure 2. The HCl-Breakthrough Curve for L-10 Pellets in a Fixed-Bed Reactor at 500°C

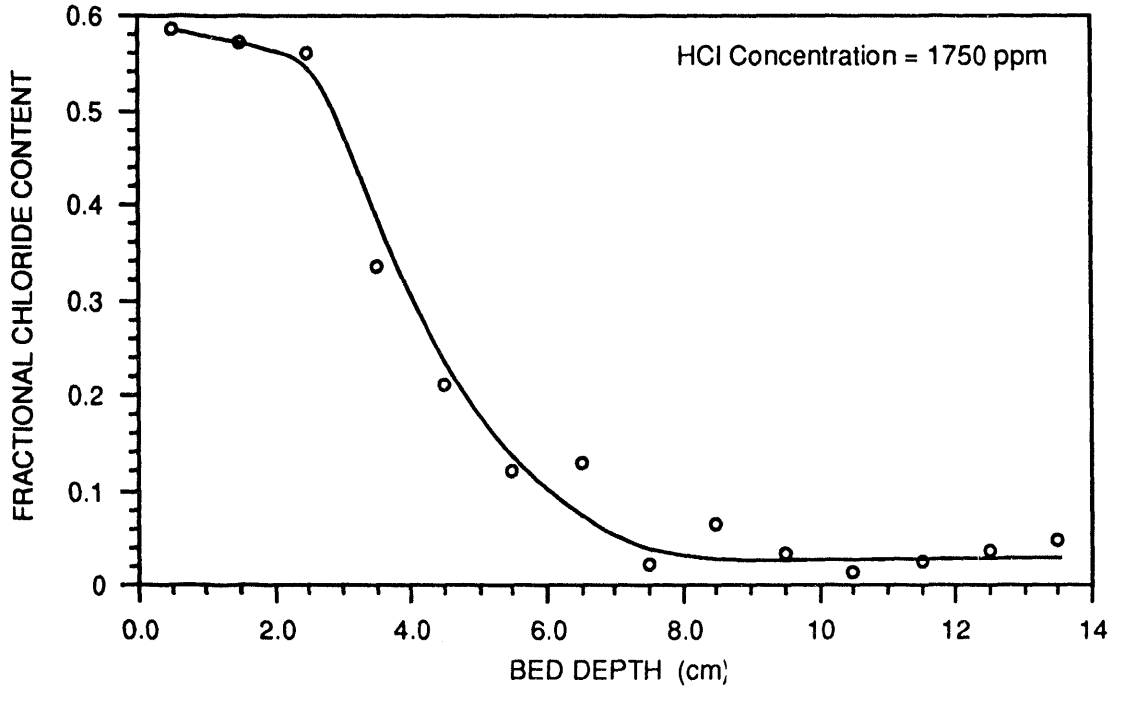

Figure 3. Distribution of Chloride in the Sorbent as a Function of Bed Depth

Table 6. Physical Properties of Granulated Nahcolite Sorbent (N-23)

Parameter	Fresh	Calcined	Spent
Surface area (m^2/g)	7.8	0.7	1.4
Bulk density (g/cm^3)	0.77	0.84	0.77
Pore volume (cm^3/g)	0.25	0.24	0.32
Median Pore Dia (μm)	0.41	1.6	1.8
Porosity (%)	36.5	36.5	39.4

Table 7. Physical Properties of Non-Granulated Nahcolite Sorbent (N-01)

Parameter	Fresh	Calcined	Spent
Surface area (m^2/g)	8.7	<0.5	<0.5
Bulk density (g/cm^3)	1.1	1.1	1.1
Pore volume (cm^3/g)	0.03	0.04	0.06
Median Pore Dia (μm)	2.9	2.0	1.9
Porosity (%)	7.2	8.2	11.5

Table 8. Results of Fluidized-Bed Experiments with Nahcolite Powder and Granules

Parameter	N-01 Sorbent at SV = 4500 h^{-1}	N-01 Sorbent at SV = 3000 h^{-1}	N-23 Sorbent at SV = 3000 h^{-1}
1-ppm breakthrough time (min)	30	720	1960
10-ppm breakthrough time (min)	40	900	2110
Chloride Capacity (wt%) at 1-ppm	0.6	9.8	25.2
Chloride Capacity (wt%) at 10-ppm	0.8	12.3	27.1

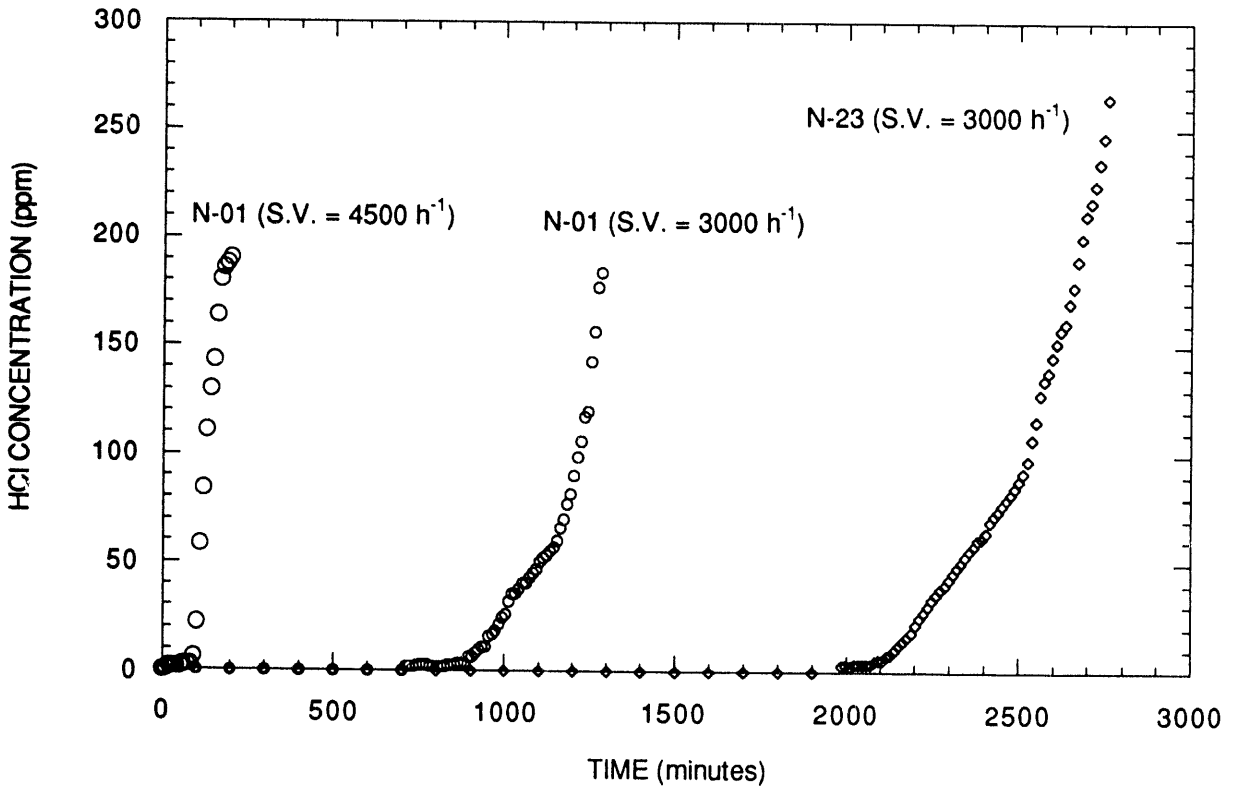

Figure 4. The HCl breakthrough curve for N-01 and N-23 sorbents in a fluidized-bed reactor at 550°C

The nahcolite sorbent particles in the size range of 45 to 90 μm were also tested for their chloride reactivity and capacity under conditions approaching an entrained-bed reactor. A gas mixture of 2.1% HCl in nitrogen was passed through the bed at a superficial gas velocity of at about 3 cm/s, slightly below the elutriation velocity of 5 cm/s for 45 μm particles. In this test, the 1 ppm HCl breakthrough time was nearly 36 h as shown in Figure 5. The experiment was continued until the HCl level reached 600 ppm. The chloride analysis of the sorbent at the end of the experiment indicated that the chloride level was 54.0 wt% at the upstream end and 37.3 wt% at the downstream end.

The above test was repeated with a simulated Texaco coal gas containing 2000 ppm HCl vapor. Under these conditions, the 1-ppm breakthrough time was nearly 435 h resulting in a chloride capacity of 51.6 wt%.

The fixed- and fluidized-bed experiments have established the following:

- The HCl vapor level was reduced consistently from about 1750 ppm to less than 1 ppm at 550°C indicating high reactivity of the sorbent for reaction with HCl.
- Chloride loading levels as high as 60 wt% were observed in the spent sorbent pellets. These results confirm the high chloride capacity of the sorbent.
- No significant loss in the crush strength was observed in pellets of spent sorbent.

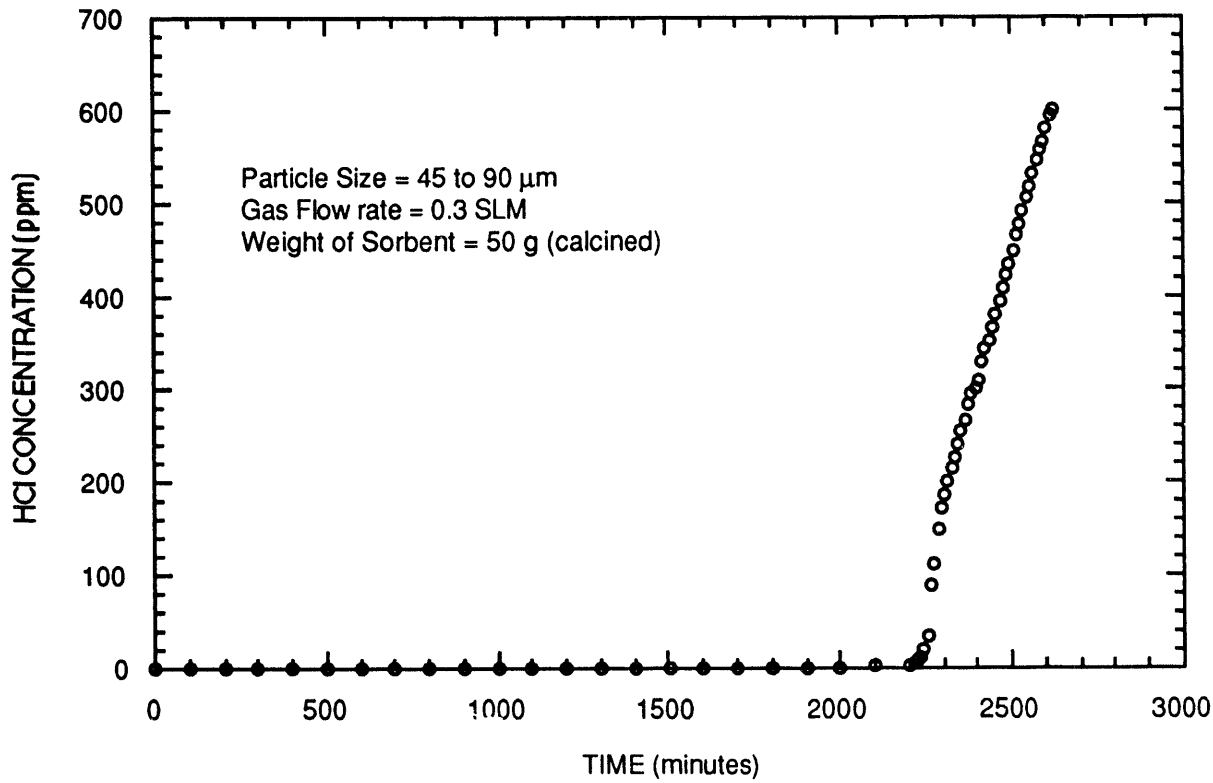

Figure 5. Removal of HCl Vapor by Non-Granulated Nahcolite at 550°C

FUTURE WORK

We will experimentally determine the suitability of other minerals such as trona and a few commercial sorbents. Additional experiments will be conducted with three suitable formulations in fixed- and fluidize-bed reactors at temperatures below 450°C and above 650°C using simulated coal-derived gas streams. Sorbent pellets suitable for moving-bed reactors will be prepared by GE-CRD and tested. A test plan will be submitted for parametric testing of one superior formulation.

Parametric tests (Task 5) will also be conducted with one superior sorbent identified in Task 4 for each type of reactor. The tests will be conducted at a minimum of three points within the ranges of interest of these critical parameters: space velocity (2,000 to 5,000 h^{-1}), temperature (480° to 750°C), and pressure (1 to 20 atm).

The experimental data will be analyzed to determine the effectiveness of the various sorbent formulations for removal of hydrogen chloride vapor in fixed-, moving-, and fluidized-bed reactors. A preliminary economic assessment is planned to determine the suitability of the sorbents for removing HCl vapor from hot coal-derived gas streams on an industrial scale.

REFERENCES

Bakker, W.T., and R.A. Perkins (1991). "The Effect of Coal Bound Chlorine on Corrosion of Coal Gasification Plant." In *Proceedings of International Conference on Chlorine in Coal*, J. Stringer and D.D. Banerjee, Eds., Elsevier.

Gillis, E. A. (1980). "Fuel Cells for Electric Utilities," Chem. Eng. Prog., **76**(10), 88.

Ham, D., A. Gelb, G. Lord, and G. Simmons (1984). "Hot-Gas Chloride Cleanup for Molten Carbonate Fuel Cells." Report No. DOE/MC/16242-1554, Morgantown Energy Technology Center, U.S. Department of Energy, Morgantown, WV.

K. Kinoshita, F. R. McLarnon and E. J. Cairns (1988). *Fuel Cells: A Handbook*, Report No. DOE/METC-88/6096, Morgantown Energy Technology Center, U.S. Department of Energy, Morgantown, WV.

Krishnan, G.N., G.T. Tong, B.J. Wood, and N. Korens (1986). "High-Temperature Coal-Gas Chloride Cleanup for MCFC Applications." Report No. DOE/MC/21167-2080, Morgantown Energy Technology Center, U.S. Department of Energy, Morgantown, WV.

Lyke, S.E., L.J. Sealock, Jr., and G. L. Roberts (1985). "Development of a Hot Gas Cleanup System for Integrated Coal Gasification/ Molten Carbonate Fuel Cell Power Plants," Report No. DOE/MC/19077-1830, Morgan-town Energy Technology Center, U.S. Department of Energy, Morgantown, WV.

Perkins, R.A., D.L. Marsh, and P.R. Clark (1990). "Corrosion in Syngas Coolers of Entrained Slagging Gasifiers." Report No. EPRI GS-6971, Electric Power Research Institute, Palo Alto, CA.

TRW (1981). "Monitoring Contaminants in Coal Derived Gas for Molten Carbonate Fuel Cells," Final Report to Argonne National Laboratory under contract No. 31-109-38-6108.

P20 PyGas Design Support

Lawrence J. Shadle, Abolghasem Shamsi,
Guo-Qing Zhang, and Edward J. Boyle
Morgantown Energy Technology Center

Yau-Hsin Wang, Madhava Syamlal, and Kalkunte Seshadri
EG&G Technical Services of West Virginia

ABSTRACT

METC is currently supporting CRS Sirrine Engineers Inc. in their development of a PyGas™ process as part of METC's implementation of the Gasification Product Facility (GPIF) project. Key issues in the gasifier have been identified and will be considered for each of the four principal sections in the gasifier: 1) the centrally located fluid bed pyrolyzer tube, 2) the top combustion and tar cracking zone, 3) the down flow co-current annular section, and 4) the counter-current fixed bed gasification zone.

The key design issues for the pyrolyzer include the desired fluidization, required conversion, size distribution of the product, the solids thru-put and residence time, and sufficient mixing in the jet to accomplish decaking of the coal. Char products from Foster Wheeler's carbonizer tests have been analyzed to evaluate the product size distribution and fluidization regime. This is compared with other fluidized bed pyrolyzers and gasifiers. A criteria for stabilizing the combustion zone and decaking the coal within the pyrolyzer jet is presented conceptually. In light of these concepts the flow patterns calculated using the MFIX code are interpreted. In addition, the characteristic times required for heating, devolatilization, and tar cracking were estimated and compared to the available residence timed to evaluate the potential for completing these processes in the pyrolyzer. Using a simple lumped analysis of this reactor some preliminary estimates for conversion in this reactor are discussed and unknowns identified.

The design issues in the top zone above the pyrolyzer include the mixing of air and steam with effluent from the pyrolyzer to achieve temperature control primarily for tar cracking. The extent of reaction of small char particles with air in this region depends on mixing and kinetics. This was evaluated using the Fluent code. Sensitivity studies were conducted assuming equilibrium predominates in this region. The results lead to the conclusion that increasing the temperature in this region has an adverse impact on gas quality.

The design issues in the co-flow section of the gasifier include the height of the bed, the rate of tar cracking and coal gasification which influence the pressure drops and exit gas temperatures. Preliminary cold flow tests suggest that small particle sizes, high gas velocities, and any compaction or tar deposition in the co-flow bed may lead to blowing out and losing the bed. These analyses have lead to the concept of flaring the inner shroud so that the cross-sectional area is larger at the exit thereby reducing gas velocities and forces leading to high

pressure drops. Tests on cracking of coal tars have been conducted using a laboratory fluid bed to evaluate the impact of char and dolomite on the rates of tar cracking. The co-flow bed was found to contribute in only a rather small portion of the total coal conversion when sensitivity studies were conducted using the MGAS code. But this impact and the final gasifier exit temperature will depend on the gasification reactivity of the char. Preliminary thermal gravimetric analysis (TGA) was used to evaluate the char reactivity and compare the observed expressions with those used for the simulations.

The counter-current fixed bed design is also based on the rate of char gasification, but the design approach assumes conservative expressions based on coke breeze and adjusted downward to account for the reduction in through-put in a conventional fixed beds when adding fines to the feed. With such fine feed materials as used in the PyGas™ fixed bed the thru-put is constrained by the gas velocity which will cause channeling or incipient fluidization. While cold flow modeling may help to define these operational limits, calculations of minimum fluidization velocity and gas flow rate as a function of conversion were used to define the useful operating regime. Gas velocities were determined from the sensitivity studies using MGAS by optimizing the air and steam to provide the highest quality gas while maintaining a peak temperature below 1260 C (2300 F) and keeping the residual carbon content in the ash below 5%.

P21 Chloride and Mercury Monitors for Air Toxics Measurements

CONTRACT INFORMATION

Contract Number	W-7405-Eng-82 (Ames) 93MC30024.000 (METC)
Contractor	Ames Laboratory Iowa State University Ames, Iowa 50011
Contractor Project Manager	William H. Buttermore
Principal Investigators	Glenn A. Norton Colin D. Chriswell
Contributing Authors	Dave E. Eckels Rachel E. Peters
METC Project Manager	Margaret A. Kotzalas
Period of Performance	October 1, 1993 - continuing
Schedule and Milestones	

FY94 Program Schedule

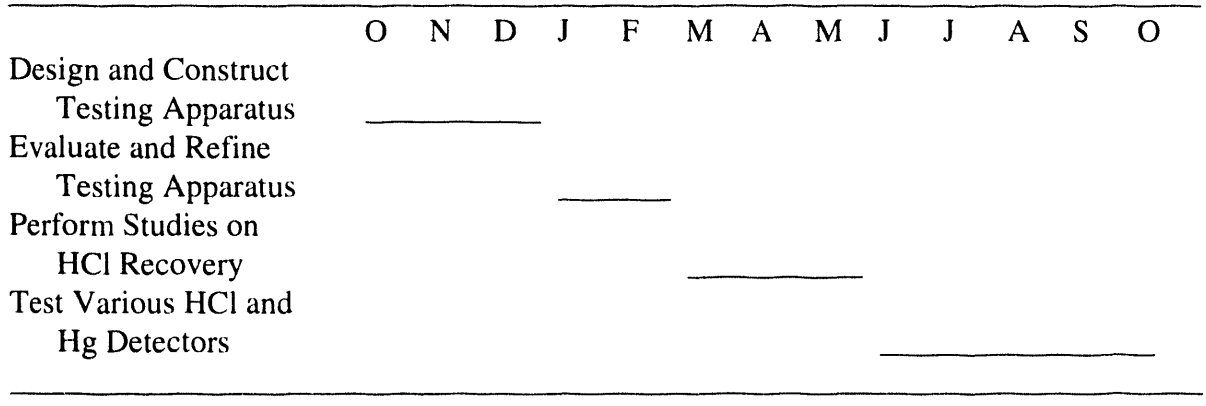

OBJECTIVES

Ames Laboratory will develop an integrated sampling and analysis system suitable for on-line monitoring of hydrogen chloride (HCl) and mercury (Hg) in advanced coal-based gasifiers. The objectives of this project are to 1) summarize current technology for monitoring HCl and Hg in gaseous effluents, 2) identify analytical techniques for such determinations in high-temperature, high-pressure gases from coal-based systems of interest to METC for producing electrical power, 3) evaluate promising analytical approaches, and 4) produce reliable on-line monitors which are adaptable to plant-scale diagnostics and process control.

BACKGROUND INFORMATION

The capability to continuously monitor and effectively control critical effluents must be developed in order to implement new clean coal technologies. Although HCl and Hg concentrations in hot, high-pressure gases from power producing systems are of environmental and technological concern, instruments suitable for determining HCl and Hg in those environments have not yet been sufficiently developed and tested. On-line analysis is more complex for such systems than for more conventional coal-based power producing systems because of the high temperatures (up to 500^{o}C) and pressures (up to 300 psi) involved. In addition, the different gas compositions involved can pose special analytical problems. Concentrations of HCl are anticipated to be in the range of 50 - 500 ppm in the raw gas and less than 1 ppm after the flue gas is treated (1-3). Concentrations of Hg are anticipated to be in the range of 0.2 - 20 ppb in the raw gas.

PROJECT DESCRIPTION

In previous work (4), commercially available instrumentation suitable for the monitoring applications of interest was reviewed and evaluated. Also, pertinent literature was assessed to obtain additional information on analytical methodologies which could potentially be used. Based on the results of that work and our continuing review of available instruments, analytical approaches which appear to have the most potential for our monitoring applications were identified.

For HCl, the techniques currently being considered are infrared absorption, colorimetry, and ion mobility spectroscopy. For Hg, atomic absorption and atomic fluorescence techniques have been selected for testing in the laboratory.

Subsequent laboratory work will determine which analytical systems show the most promise for on-line analysis of HCl and Hg. Promising analytical instruments (or components of instruments) will be assembled and/or modified for application to monitoring hot pressurized gases from coal gasifiers. Additional work will involve developing suitable gas conditioning and sample introduction systems. That work may be as important as the development of the analytical systems themselves. After the laboratory studies have been completed, prototype instruments will be tested and evaluated in the field.

RESULTS

Testing Apparatus

A laboratory apparatus was designed and constructed to blend, heat, and deliver gases to simulate gasifier streams. That apparatus will be used to study sample delivery and to evaluate various detectors. The basic design consists of a Teflon gas mixer for blending metered gases, a

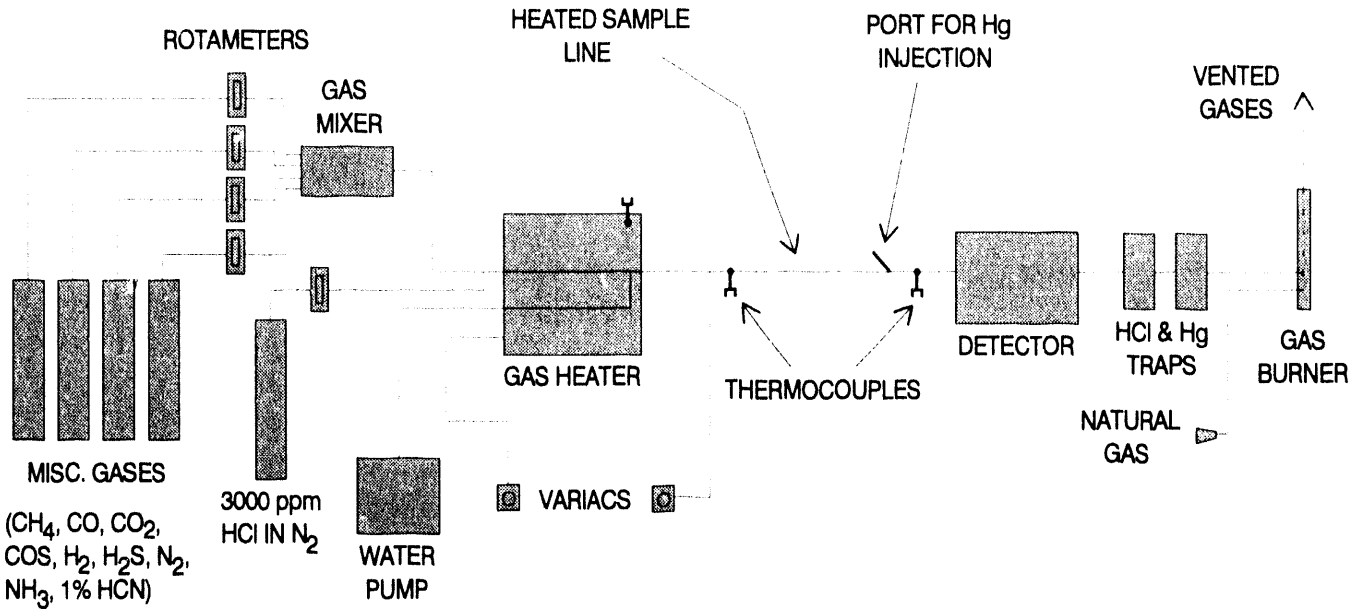

Figure 1. Testing Apparatus for Evaluating HCl and Hg Analyzers

gas heating system, a steam generator, toxic gas traps (to be used after the detector), and a gas burner for burning flammable gases and destroying toxic gases not collected by the traps. The tubing from the HCl gas cylinder is made of Teflon, while all the other gas lines are made of stainless steel. A schematic diagram of the current testing apparatus is shown in Figure 1.

After assessing the overall operation of the initial system, modifications or alternate approaches in the steam generation, gas heating, and gas burner components were made. Some of those changes included replacing a gas chromatography oven with a hot sand bath to heat the gases. The blended gases are heated by passing them into a stainless steel coil immersed in the sand bath. To achieve a gas temperature of about 200°C, the sand bath is maintained at 300-400°C. In addition, an external steam generation vessel was replaced with a pump from a liquid chromatograph (LC). The LC pump provides a precise, adjustable water flow in the proper range to give the desired moisture content in the sample gas mixtures. The water is pumped into a separate stainless steel coil in the hot sand bath. The water is vaporized in the steam coil and is introduced into the sample gas stream just before the sample gases exit the sand bath.

HCl Studies

Preliminary studies were initiated to determine whether a known amount of HCl can be reliably delivered to a detector. Initial tests involved recovering HCl directly from a cylinder containing a HCl gas mixture (3000 ppm_v in nitrogen). Recoveries were determined by bubbling the gas into an absorbing solution and then titrating the solution to determine the amount of chloride collected. Erratic results and low recoveries were obtained at relatively low gas flows (e.g., 10 cm^3/min), even when using Teflon lines directly from the gas cylinder. The erratic results do not appear to be caused by

analytical errors, problems in collection efficiency, gas metering errors, or losses in the Teflon line. Rather, there appears to be erratic adsorption/desorption processes occurring upstream from the regulator outlet, despite the precautions taken to select a regulator with nonreactive components. Good precision for HCl recoveries was obtained by increasing the gas flow rates to 100 cm^3/min or more.

Subsequent tests involved passing the HCl gas mixture through the entire testing apparatus. Those tests were performed both with heated (180-200°C) and unheated gases. In the former case, tests were also performed with and without about 50% water present in the gas stream. A total of about 25 tests were performed using HCl/N_2 gas flows of 100-550 cm^3/min. Overall, HCl recoveries averaged 86 ± 5%. The best precision and recoveries were observed for the tests where water vapor was present, in which case the HCl recovery averaged 92 ± 3%.

An alternate approach for delivering known amounts of HCl was investigated. In that approach, a dilute aqueous hydrochloric acid solution is pumped at a known rate into a stainless steel coil in a hot sand bath. The hot coil vaporizes the HCl and water, which are then introduced to the primary gas stream in a heated sample line. By varying the water flow rate and the HCl concentration in the water, it should be possible to obtain both the desired moisture and HCl gas concentrations in the delivered gases. Good recoveries and precision were obtained in some cases. However, pumping problems were encountered when attempting to use the low flows necessary to attain both the desired H_2O and HCl concentrations at the total gas flow rate (about 1 liter/min) being tested. Efforts in this area have been discontinued since the HCl gas mixture appears to be working satisfactorily.

We have begun contacting various companies in an attempt to borrow the detectors of interest. These include one colorimetric detector and two different gas filter correlation IR units. In addition, we are now performing our final screening of Fourier transform IR detectors and ion mobility spectrometers. One or two detectors from each of the latter analytical approaches will also be selected for study.

Hg Studies

In preparation for later tests involving Hg determinations, some preliminary studies were performed to study potential problems in analyzing Hg using conventional instruments and standard procedures. One potential calibration technique is to inject Hg vapors (using gas-tight syringes) into the sample gas stream. The validity of using that approach was experimentally confirmed.

Studies were also performed using liquid Hg standards. Minor procedural variations were found to significantly affect the amount of Hg detected in those standards. In particular, when and how the standards are acidified during preparation were found to be important variables. By carefully controlling those and other variables, full recoveries of 100-ng quantities of Hg in liquid standards can now be consistently obtained. That work will be important when verifying the operation of a Hg permeation tube calibration system which will be used to compare different Hg detectors.

A final review of potential instruments for use in an on-line monitor was made. Measurements based on resistance changes in a gold film originally appeared promising. However, after continued discussions with company representatives, it became evident that the gold film approach is probably not a method of choice at this time. This is largely due to the costs and logistics associated with the frequent off-line calibrations which would be required for continuous analyses of gas streams. Consequently, that approach is no longer being

considered for on-line monitoring of coal gasifier streams.

Two atomic absorption detectors and one atomic fluorescence detector have been selected for study in our laboratories. Contacts with the pertinent companies have been initiated in an attempt to acquire the detectors of interest as short-term cost-free loans. Brief acquisitions of those instruments will allow us to make valid, direct instrument comparisons. This will in turn help us select the best instrument for use in an on-line Hg analyzer.

FUTURE WORK

Studies on the delivery of known amounts of HCl from our testing apparatus will continue. In this regard, the effects of gas temperature, gas stream composition, and flow rate on HCl recovery will be studied in more detail. HCl recovery will be examined while the entire testing apparatus is in operation and while all of the gases selected to simulate coal gasifier streams are flowing through the system. After those tests, our laboratory evaluation of selected HCl detectors will begin.

For Hg, a permeation tube calibration system and manual injections of Hg vapor (using gas-tight syringes) will be used to evaluate various detectors. Testing will be performed both with and without the use of gold amalgamation for collecting and concentrating Hg prior to analysis. A double gold amalgamation approach may also be integrated into the analytical system and tested as a possible approach for improving accuracy and precision.

For both HCl and Hg, subsequent testing will include determining the effects of gas temperature, pressure, and composition (including moisture content) on detection limits, dynamic range, precision, and accuracy. The effects of sample line composition will also be studied. Modifications of existing instruments will be made, as needed, for application to gasifier streams.

The severity of interferences from compounds such as H_2S, CH_4, HF, and H_2O on HCl and Hg determinations will be investigated. In addition, suitable sample handling systems will be developed. Gas conditioning steps which may be required include temperature and pressure adjustments, filtering particulate matter, and removing moisture and interfering gases. The amount and type of gas conditioning will be largely dependent on the analytical methodology employed. Ultimately, prototype analytical systems which appear to be acceptable based on results of laboratory studies will be integrated with the gas handling system and then tested in the field.

ACKNOWLEDGEMENTS

This work was performed with funds provided by the U.S. Department of Energy through the Morgantown Energy Technology Center. Ames Laboratory is operated for the U.S. D.O.E. by Iowa State University under Contract No. W-7405-Eng-82.

REFERENCES

1. G. N. Krishnan, G. T. Tong, B. J. Wood, and N. Korens, "High Temperature Coal Gas Chloride Cleanup for Molten Carbonate Fuel Cell Applications," Final Report, DOE/MC/21167-2080 (DE87001041), November 1986, pp. 57-60.

2. G. L. Anderson, F. O. Berry, B. D. Harmon, R. M. Laurens, and R. Biljetina, "Development of a Hot Gas Cleanup System for Integrated Coal Gasification/Molten

Carbonate Fuel Cell Power Plants," Final Report, DOE/MC/19403-1816 (DE86001589), October 1985, p. A-4.

3. T. Grindley and T. H. Gardner, "Trace Contaminants in Fixed-Bed Gasifier Gas," in Proc. Twelfth Annual Gasification and Gas Stream Cleanup Systems Contractors Review Meeting, Volume II, DOE/METC-92/6128, Vol. 2 (DE93000229), September 1992, pp. 479-497.

4. G. A. Norton, C. D. Chriswell, D. E. Eckels, and W. H. Buttermore, "On-Line Monitoring of Mercury and Hydrogen Chloride in Hot Gases from Coal Gasifiers," in Proc. Coal-Fired Power Systems 93 -- Advances in IGCC and PFBC Review Meeting, DOE/METC-93/6131 (DE93000289), June 1993, pp. 276-283.

P22 Cooperative Research and Development Agreements at METC

J. Christopher Ludlow, Lisa A. Jarr, and William F. Lawson
Morgantown Energy Technology Center

ABSTRACT

With the passage of the Federal Technology Transfer Act of 1986, the Morgantown Energy Technology Center (METC) was empowered and encouraged to enter into joint research and development projects that would transfer fossil energy technologies into the private sector. Potential partners for these joint projects, formalized by a Cooperative Research and Development Agreement (CRADA), include private industry, educational institutions, and other research organizations. Development of CRADA with METC is a simple process. In a CRADA, both the Government and the participating partner(s) may contribute personnel, equipment, or facilities to the project but no funds may be supplied by the Government to the other party. Also facilitating working with the Government is the fact that METC's Director is able to negotiate directly with the partners on intellectual property issues including the exclusive licensing of METC inventions, protection of proprietary data, and allocation of patent rights developed under the agreement.

P23

Optimal Design and Synthesis of Advanced Power Systems under Uncertainty

Urmila M. Diwekar & Edward S. Rubin
Carnegie Mellon University
Pittsburgh, PA 15213

H. Christopher Frey
North Carolina State University
Raleigh, NC 27695

Abstract

Technical and economic uncertainties are not rigorously treated or characterized in most preliminary cost and performance estimates of advanced power system designs. Nor do current design methods rigorously address the issues of design under uncertainty. However, process costs and other important quality measures, such as controllability, safety, and environmental compliance, largely depend on the process synthesis stage. This conceptual design stage involves identifying the basic flowsheet structures from a typically large number of alternatives. This paper describes the status of on-going research at Carnegie Mellon University to develop and demonstrate advanced computer-based methods for dealing with uncertainties that are critical to the design of advanced coal-based power systems. Preliminary results are presented illustrating the use of these new modeling tools for the environmental control design of an advanced integrated gasification combined cycle (IGCC) system using hot gas cleanup. Additional applications to pressurized fluidized bed combustion (PFBC) and externally-fired combined cycle (EFCC) systems are in progress.

1 Introduction

Increasing environmental awareness and regulations have placed new requirements on process design for advanced power systems, and increased the need for sophisticated simulation and design tools for examining pollution prevention options. The conventional process models now in use are largely based on a deterministic framework used for simulation rather than process synthesis. An important shortcoming of these models is the ability to analyze uncertainties more rigorously. Such capability is especially important in the context of advanced energy systems, since available performance data typically are scant, accurate predictive models do not exist, and many technical as well as economic parameters are not well established.

Though design under uncertainty has received considerable attention in the chemical engineering literature during the past few years a generalized framework for analyzing uncertainty systematically has only recently been developed around a chemical process simulator (Diwekar and Rubin, 1991). This capability has been used successfully for the evaluation of different configurations of integrated gasification combined cycle (IGCC) systems, which represent a clean and efficient use of coal for electric power generation. In previous work we have applied probabilistic methods to evaluate the performance, cost, and emissions from IGCC systems, compare alternative systems with uncertainty, and the benefits from targeted R & D (Frey and Rubin 1992a, 1992b; Frey, et al., 1994).

In the present project, we enhance this framework through development of a generalized capabil-

ity to deal with process synthesis and optimization as well as with stochastic optimization and stochastic programming problems. Sequential-modular simulators like ASPEN and PRO/II have grown in sophistication over the years and are widely used in the chemical industries to solve complex problems with rigorous process modeling. Therefore, it is desirable to build the new process synthesis and stochastic optimization capability around such simulators. Such capabilities have been built around the public version of ASPEN simulator developed for DOE (MIT, 1982). First we describe the methodological basis for the new modeling capabilities. Then we present an illustrative case study of their application to power systems design.

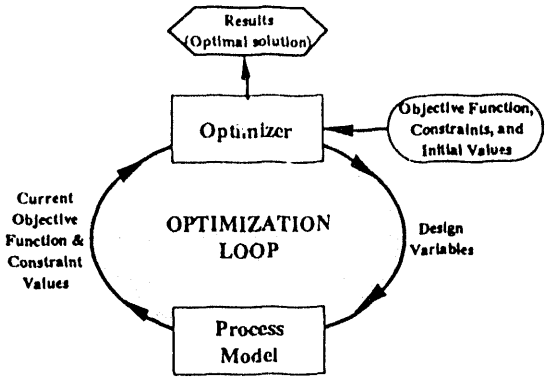

Figure 1: Pictorial Representation of the Optimization Framework

2 Methodology for Stochastic Optimization and Optimal Design under Uncertainty

The various problems reported in the literature on stochastic optimization/programming, and chemical process design under uncertainty are divided into two categories: 1) stochastic optimization, and 2) stochastic programming. The "here and now" problems involving expected value minimization, the chance constrained optimization problem, and the design for optimal flexibility problem all require that at each optimization iteration some probabilistic representation of the objective function and constraints is optimized. These problems are classified as stochastic optimization problems. On the other hand, the "wait and see," "flexibility index," and multiperiod optimization problems involve solution of a deterministic optimization problem for each scenario so that one gets a probabilistic representation of optimal solutions. These type of problems are considered under the category of stochastic programming, namely the effects of uncertainties on optimal design. This new division makes it easier to generalize the use of the new modeling capability for different kinds of optimization problems under uncertainty, and to design a uniform framework for solving large-scale problems.

2.1 The Optimizer

The goal of an optimization problem is to determine the decision variables x that maximize some aspect of the deterministic model represented by the objective function Z, while ensuring that the model operates within established limits enforced by the equality constraints h and inequality constraints g. A generalized statement of this problem is given by the following equation.

$$\underset{x}{\text{Optimize}} \quad Z = z(x) \tag{1}$$

subject to

$$h(x) = 0 \tag{2}$$

$$g(x) \leq 0 \tag{3}$$

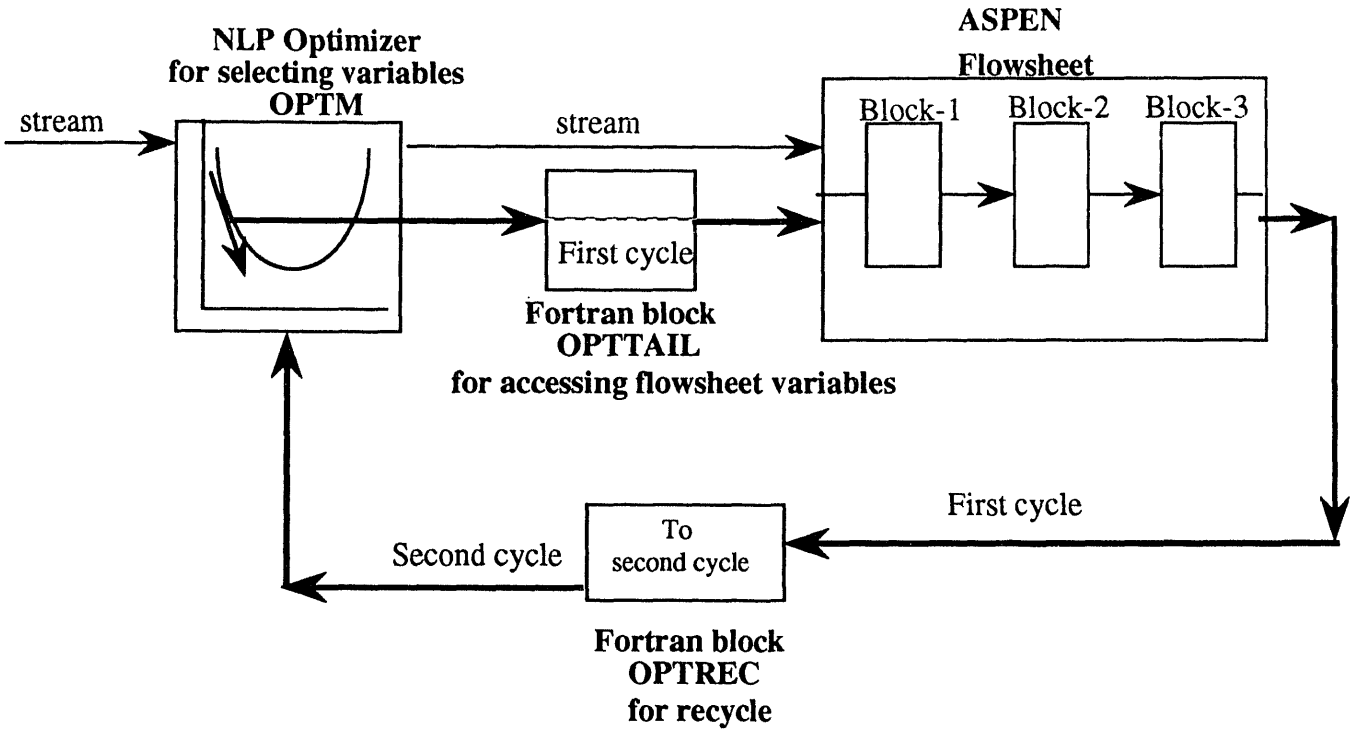

Figure 2: Basic Operation of the ASPEN Optimizer

where x is a decision variable vector. The above formulation represents the deterministic optimization problem, for which a generalized iterative solution procedure is illustrated schematically in Figure 1 and the ASPEN implementation in Figure 2. As seen in the figure, the optimizer invokes the model with a set of values of decision variables x. The model simulates the phenomena and calculates the objective function and constraints. This information is utilized by the optimizer to calculate a new set of decision variables. This iterative sequence is continued until the optimization criteria pertaining to the optimization algorithm are satisfied. In this case the model which is used is deterministic in nature.

The optimizer block, OPTM, in Figure 2 has been implemented in ASPEN as a unit operation block. The OPTM block is a flowsheet optimization block which solves the nonlinear optimization problem (NLP) described above.

Recent advances in constrained nonlinear optimization techniques provide better choices for solving large scale flowsheet problems. The most popular of these methods are generalized reduced gradient (GRG) and successive quadratic programming (SQP), and their variants. Among generalized reduced gradient methods, the most widely used algorithms are GRG2 and MINOS (Gill et al., 1981). Most literature on large scale optimization favors the SQP method because the GRG2 algorithm requires convergence of equality constraints at each iteration. Furthermore, historically the GRG strategy has been considered to be the less efficient mode of optimization (Biegler, 1983). Hence the GRG2 algorithm is not well suited for the large scale optimization problems we are proposing to address. On the other hand, MINOS does not require convergence of equality constraints, and is best suited for optimization problems with linear constraints.

SQP is the most widely used technique for large scale nonlinear optimization for chemical processes, which typically involve highly nonlinear models. In SQP, at each iteration the problem is approximated

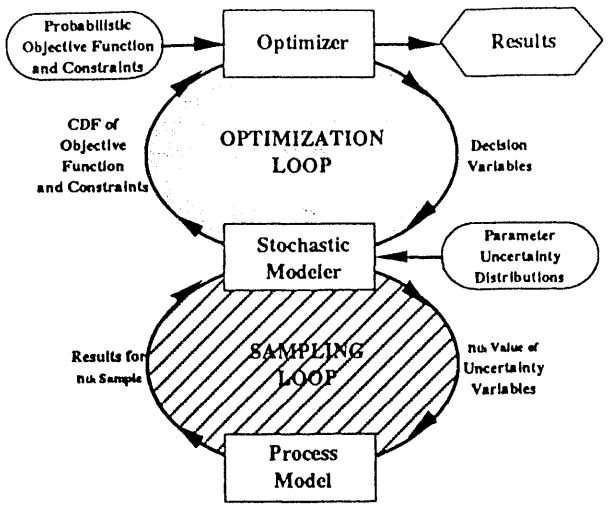

Figure 3: Pictorial Representation of the Stochastic Optimization Framework

as a quadratic program where the objective function is quadratic and the constraints are linear. Similar to linear programming, the special features of a quadratic objective function are exploited to solve the problem more efficiently. The quadratic programming subproblem is solved for each step to obtain the next trial point. This cycle is repeated until the optimum is reached.

In Figure 2, the NLP optimization block, OPTM, generates decision variable sets using the SQP method (Biegler and Cuthrell, 1985). This set is passed to the flowsheet using a Fortran OPTTAIL block. After the simulation run, the values of the objective function and constraints are calculated using the OPTREC block and passed to the OPTM block. The iterations stop when the best improvement to the process for the defined objective function and constraints is found. The modular nature of both the stochastic and optimization blocks allow one to solve different stochastic optimization and stochastic programming problems encountered in practice. The following subsection describes this functionality.

2.2 Stochastic Optimization

In many cases, including advanced energy conversion technologies, the model builder cannot ignore the uncertainties associated with some of the model input parameters. An uncertainty analysis thus becomes essential. As uncertainty is a broad concept, it is possible—and often useful—to approach it in several different ways. One rather general approach, which has been described earlier and successfully applied to a wide variety of problems, is to assign a probability distribution to the various uncertain or variable parameters (Diwekar and Rubin, 1991).

The generalized stochastic optimization problem, where the decision variables and uncertain parameters are separable, can then be viewed as:

$$\underset{x}{\text{Optimize}} \quad P1(Z) = P1(z(x,u)) \tag{4}$$

subject to

$$P2(h(x,u)) = 0 \tag{5}$$

$$P3(g(x,u) \leq 0 \tag{6}$$

where u is the vector of uncertain parameters and the P represents the probabilistic functional which for an expected value minimization reduces to:

$$E(F(u)) = \int_0^1 F(u)dp(u). \tag{7}$$

This function can be calculated by sampling the function and calculating the expected value of the samples.

$$E(F(u)) = \frac{\sum_1^{N_{samp}} F(u)}{N_{samp}} \tag{8}$$

On the other hand, in the case of chance constrained optimization the constraints are represented

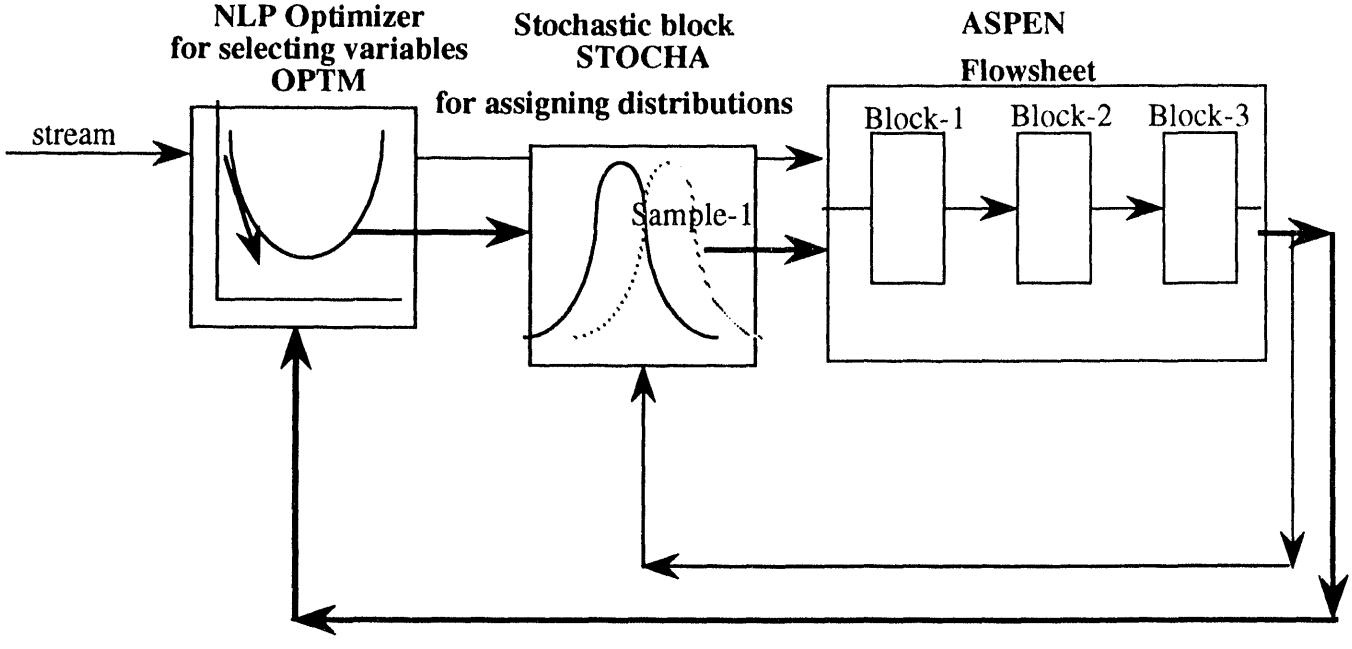

Figure 4: Schematic of the Stochastic Optimization Framework in ASPEN

in terms of a probability of exceeding certain value and is represented by:

$$\underset{x}{\text{Optimize}} \quad P1(z(x,u)) = E(F(u)) \qquad (9)$$

subject to

$$P(h(x,u) > \beta) \leq P_c \qquad (10)$$

where Equation 10 is the chance constraint.

It is apparent from the above discussion that unlike the deterministic optimization problem, in stochastic optimization one has to consider the probabilistic functional of the objective function and constraints. The generalized treatment of such problems is to use probabilistic or stochastic models instead of the deterministic model inside the optimization loop.

Figure 3 represents the generalized stochastic optimization problem solution procedure where the deterministic model in Figure 3 is replaced by an iterative stochastic model. Figure 4 illustrates the ASPEN implementation.

This stochastic optimization capability can also be used to achieve off-line quality control. In off-line quality control, the sensitivity of the design to the sources of variation is reduced at the design stage to make the controller design easier. One such approach based on the concept of Taguchi's parameter design method has been illustrated using the above-mentioned stochastic optimization capability (Diwekar and Rubin, 1994). This approach involves minimizing the variance of the objective function instead of the expected value.

2.3 Effect of Uncertainties on Optimal Design

In contrast to the stochastic optimization problems, which involve expected value minimization, and the chance constrained problems, the "wait and see,"

and multiperiod optimization problems are categorized as stochastic programming problems. The "wait and see" problem involves deterministic decisions at each random stage or random sample, which is the same as solving multiple deterministic optimization problems, and can be represented as:

$$\underset{x}{\text{Optimize}} \quad Z = z(x, u*)) \tag{11}$$

subject to

$$h(x, u*) = 0 \tag{12}$$

$$g(x, u*) \leq 0 \tag{13}$$

where $u*$ is the vector of values of uncertain variables corresponding to some sample. This optimization procedure is repeated for each sample of uncertain variables u and a probabilistic representation of outcome is obtained. Figure 5 represents the generalized solution procedure where the deterministic problem shown in Figure 3 forms the inner loop, whereas the stochastic sampling forms the outer loop. This procedure is implemented in the ASPEN simulator as shown in Figure 6. From the ASPEN representation, it is clear that by just interchanging the position of stochastic block, STOCHA, and the optimization block, OPTM, one can solve almost all the problems in the stochastic optimization/programming literature.

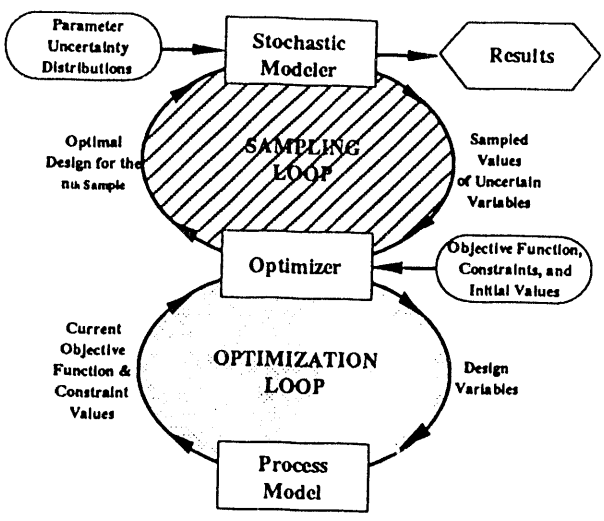

Figure 5: Pictorial Representation of the Stochastic Programming Framework

3 Methodology for the New Process Synthesis Capability

The alternatives for process design and environmental control often are numerous and involve a very large search space. Selection of the best alternatives can offer the potential for significantly reducing costs and/or improving performance. Therefore, there is a strong need for "systems" research to identify the best ways of configuring advanced energy systems. The current state of process synthesis techniques involves: (a) the heuristic approach which

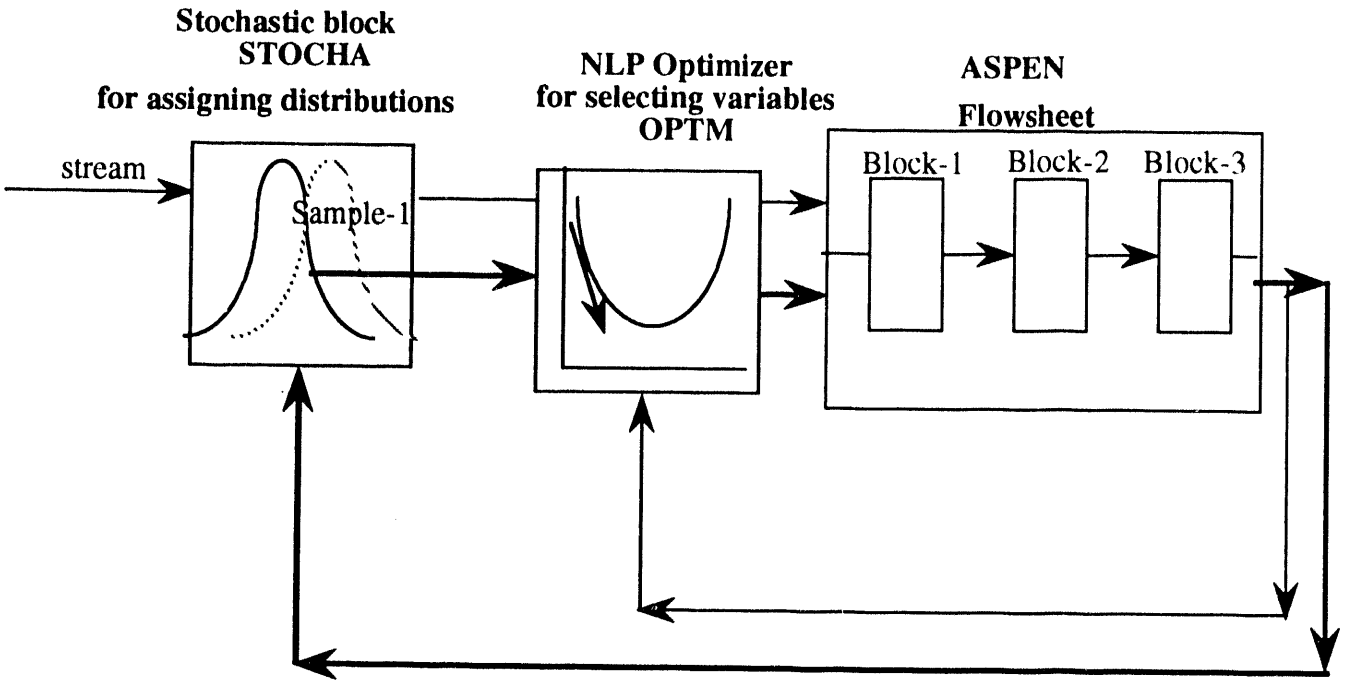

Figure 6: Schematic of the Stochastic Programming Framework in ASPEN

relies on intuition and engineering knowledge, (b) the physical insight approach which is based on exploiting basic physical principles, and (c) the optimization approach which uses the mathematical programming techniques. This section deals with a newly developed process synthesizer built around the public version of ASPEN, using the mathematical programming approach (Diwekar et al., 1991).

3.1 The Mathematical Programming Approach

The mathematical programming approach to process synthesis involves:

(a) Formulation of a flowsheet superstructure incorporating all the alternative process configurations.

(b) Modeling the superstructure as a mixed integer nonlinear programming (MINLP) problem of the form

MINLP:

$$Z = \min_{\overline{x}, \overline{v}, \overline{y}} \quad c^T\overline{y} + f(\overline{x}, \overline{v}) \tag{14}$$

subject to

$$\begin{aligned} h(\overline{x}, \overline{v}) &= 0 \\ h1(\overline{x}, \overline{v}) &= v - z(\overline{x}) = 0 \\ B^T\overline{y} + g(\overline{x}, \overline{v}) &\leq 0 \\ y \in Y;\ x &\in X \end{aligned} \tag{15}$$

where

$$Y = [y|Ay \leq a,\ y[0,1]^m]$$

$$X = [x|x^L \leq x\ le\ x^U]$$

The continuous variables x represent flows, operating conditions, and design variables. The variables v are the output variables which are

related to the input variables x by model equations. For equation oriented environments, these model equations are embedded in the equality constraints $h1(\bar{x}, \bar{v})$. The binary variables y denote the potential existence of process units.

(c) Identification of both the optimal configuration and operating process parameters by an algorithm based on alternating sequence of nonlinear programs (NLPs) and mixed integer linear programs (MILPs).

3.2 The ASPEN MINLP Process Synthesizer

The MINLP process synthesis capability in the public version of ASPEN is based on ZOOM (Marsten, 1986), the mixed integer linear programming (MILP) solver, and on SCOPT (Lang and Biegler, 1987), the nonlinear programming (NLP) solver. The method is based on an algorithm called GBD/OA/ER/AP presented by Diwekar et. al (1992) which involves solution of alternate sequence of MILP and NLP problem solving. The overall structure of the environment is shown in Figure 7. Optimization of the MINLP process synthesis problem is decomposed into continuous optimization of NLP problems at fixed choice of binary variables, and discrete optimization through the MILP master problem. The MILP solver (Master) and NLP optimizer have been implemented in ASPEN as unit operation blocks and can be executed easily with the ASPEN process unit blocks.

The process synthesis environment in ASPEN consists of the Master block, the NLP optimizer, and the entire superstructure. The initialization of the continuous and binary variables is done in the ASPEN input file. At this stage the scheme is translated into an initial flowsheet and subsystems using the decomposition strategy of Kravanja and Grossmann (1990). NLP optimization of the selected flowsheets is the first step in the inner loop, which results in the objective function and linearization information.

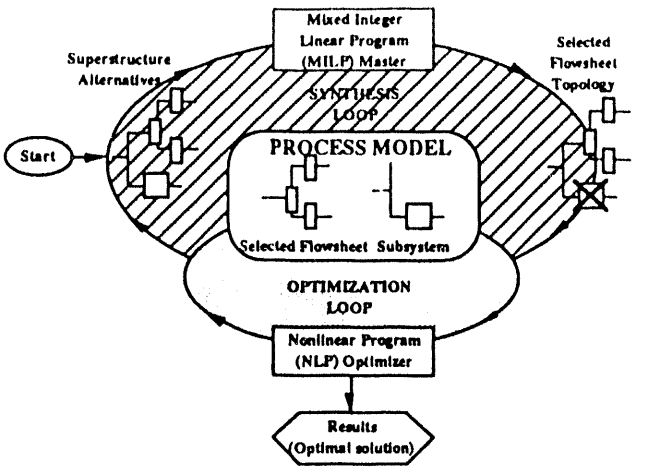

Figure 7: Schematic of the New ASPEN MINLP Synthesizer

This information is passed to the Master block which internally modifies the master problem to include the linearization information. The solution of the master problem results in a new flowsheet structure. The iteration stops when there is no improvement in the objective function value.

3.3 The Implicit Constraint Problem

The implementation of this new capability in a sequential modular simulator poses challenging problems which are not encountered in equation-oriented simulators; therefore, new strategies are necessary to solve these problems. One such problem associated with the MINLP sequential modular process synthesizer is that of *implicit constraints*.

The problem of implicit constraints is encountered because of the black box nature of the models in sequential modular simulators. The ASPEN MINLP environment is based on a two-level op-

timization algorithm consisting of an upper level MILP master problem and a lower level NLP problem. The MILP master problem predicts new binary variables, while the NLP problem provides new continuous variables. The MILP master problem represents the linearized NLP problem with non-fixed binary variables, since at each stage the MILP master problem obtains the linearization information from the NLP optimizer. Unlike equation oriented simulators, in sequential modular simulators most of the nonlinear constraints are not represented explicitly by equations. The linearization information on these constraints, which are essentially black box relations embedded in the simulator environment ($h1(\bar{x},\bar{v})$ in equation 2), therefore must be passed to the master problem.

In order to circumvent this problem of implicit constraints new decision variables are created. These are equated to the output variables from the flowsheet configurations. This procedure ensures that the original MINLP problem remains the same, while at each stage the MILP master problem receives increased information from the NLP optimizer. Although this procedure assures complete information transfer to the master problem, it also increases the computational load on the NLP optimizer, which is generally the rate-determining step in the MINLP process synthesis. Recently Diwekar and Rubin (1993) presented a partitioning strategy which reduces the computational load on the NLP problem crucial for the solution of large-scale synthesis problems.

4 Illustrative Examples of New Modeling Capabilities

The new capabilities for process synthesis and optimization under uncertainty provide powerful new tools for the design and analysis of advanced energy systems. An application of the new synthesis capability already has been described in a recent paper (Diwekar, et al., 1992), which focuses on choosing a least-cost approach to sulfur removal for an IGCC system with hot gas cleanup and a fluidized bed gasifier. In this paper we show new results that illustrate use of the stochastic optimization and stochastic programming capabilities for the design of a different IGCC system.

To illustrate these new capabilities, an air-blown dry ash Lurgi gasifier IGCC system flowsheet with a plant size of 650 MW and a high-sulfur Illinois No. 6 coal is analyzed. A schematic of this technology is shown in Figure 8. The hot gas cleanup system features high temperature (1100 degrees F) sulfur removal from the fuel gas with a zinc ferrite sorbent, and high efficiency cyclones and ceramic filters for particulate removal. Details of the performance and cost models are reported elsewhere (Frey and Rubin 1992a).

Two key design variables for the fixed bed zinc ferrite process are the sulfur absorption cycle time and the reactor vessel length-to-diameter ratio. The sulfur absorption cycle time is constrained to be at least as great as the time required to regenerate a bed of sulfated sorbent and return it to active service after a regeneration cycle. As the sulfur absorption time becomes longer, more sorbent is required to capture the syngas sulfur species over the increased time period. Larger absorption cycle times therefore require either larger reactor vessels and/or more reactor vessels. The length-to-diameter ratio of the reactor vessel also affects process economics.

Another key area of uncertainty for this technology is the NO_x emission rate. Thermal NO_x emissions are expected to be quite low for IGCC systems due to the low heating value of the fuel gas and the presence of thermal diluents such as H_2O, CO_2, and N_2 (Holt et al., 1989). However, the hot gas cleanup system employed by the air-blown Lurgi system does not remove fuel-bound nitrogen (in the form of ammonia) from the fuel gas, and a substantial portion of the ammonia is converted to NO_x upon combustion. Thus, NO_x emissions pose a critical concern for systems with hot gas cleanup. For example, using conventional com-

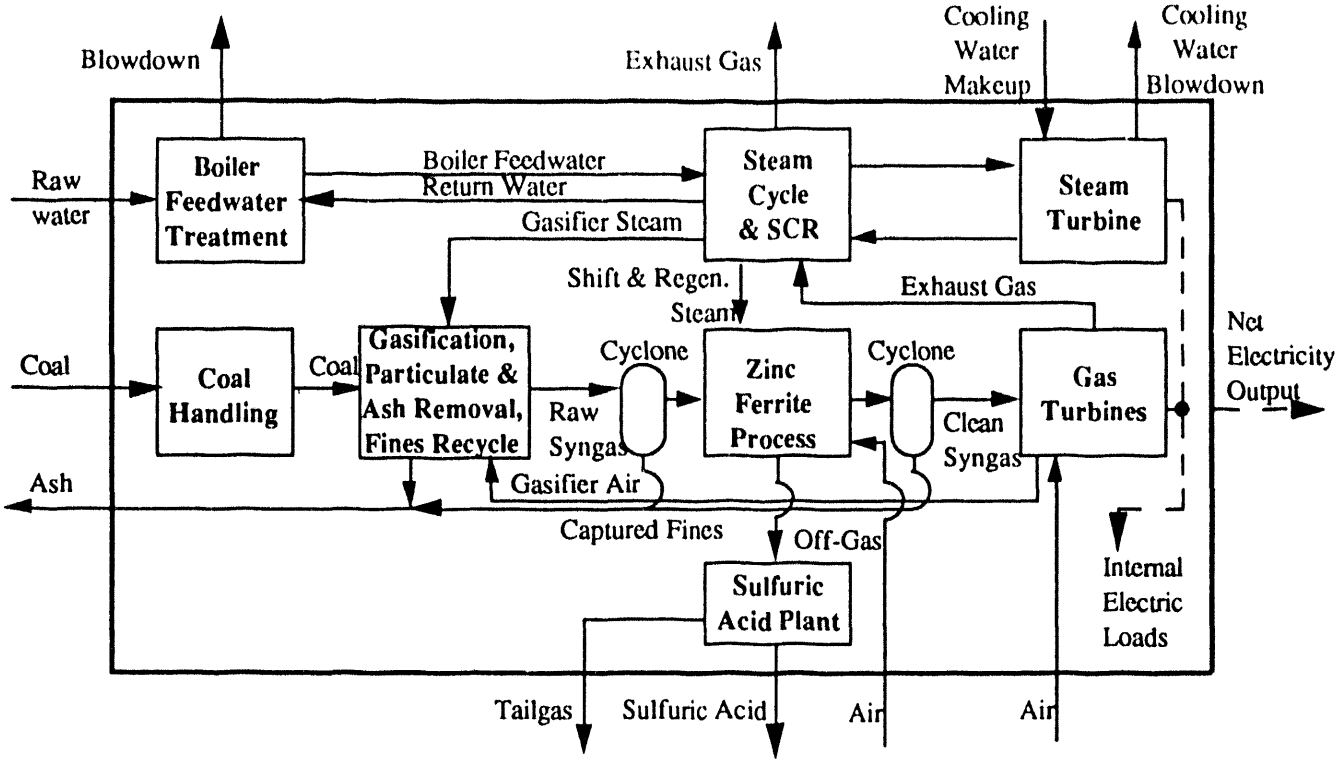

Figure 8: Schematic of the Lurgi Air-blown Dry Ash Gasifier IGCC System

bustors the DOE/METC performance model yields NO_x emissions nearly four times greater than federal New Source Performance Standards (NSPS) for coal-fired power plants.

To mitigate NO_x emissions, several approaches are possible. In the near term, the most likely approach is the use of post-combustion exhaust gas NO_x reduction technology. In the longer term, advanced staged combustion designs, featuring rich/lean combustion, may be commercialized and employed for fuels with high nitrogen content. In this study, we consider the use of selective catalytic reduction (SCR) for NO_x control. In a SCR system, ammonia is injected into the flue gas upstream of a catalytic reactor through a set of nozzles comprising an injection grid. Because of the temperature window required for typical SCR catalysts, the SCR reactor employed with gas-turbine combined cycle system are typically located in the heat recovery steam generator (HRSG). We employ a new performance and cost model of an SCR system (Frey, 1993) to explore the effects of two key design variables: the required NO_x removal efficiency, which has a substantial impact on the catalyst volume requirement, and the catalyst layer replacement interval, which can be varied to achieve trade-offs between initial capital cost and annual replacement costs for catalyst.

Key performance and cost parameters of the engineering models for the IGCC system were assigned probability distributions based on data analysis, literature review, and the elicitation of expert judgments.

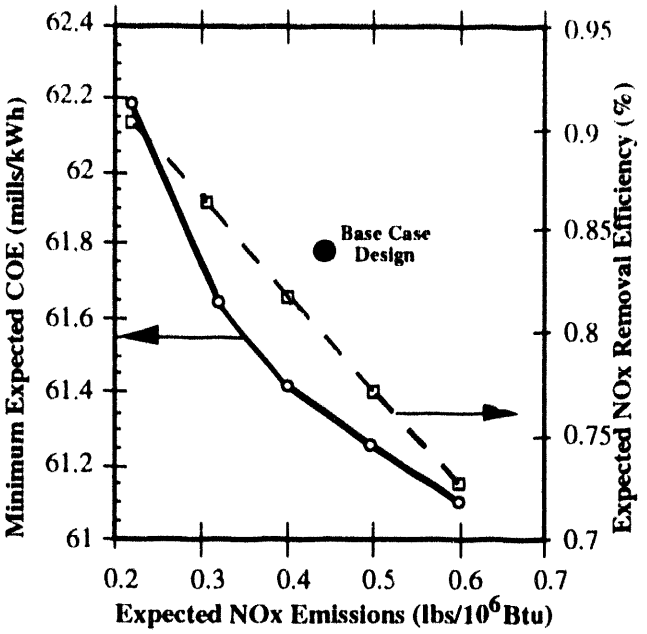

Figure 9: Minimization of Expected Cost of Electricity Subject to Expected Value of NOx Emission Constraints.

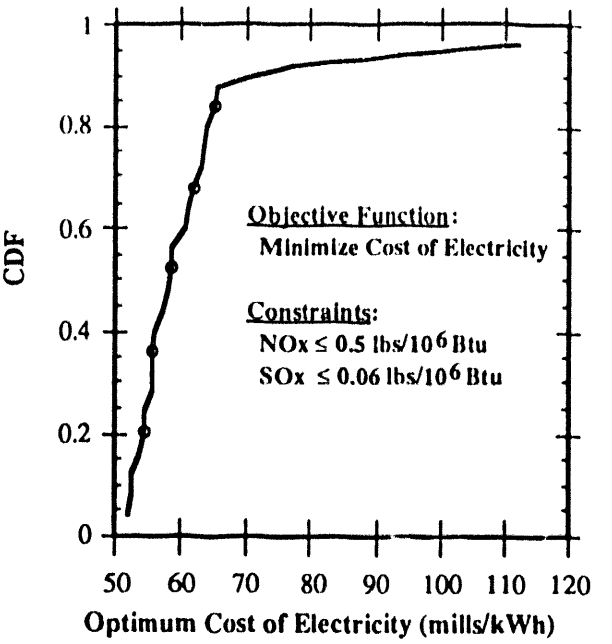

Figure 10: Effect of Uncertainties on Minimum Cost.

The characterization of performance uncertainties focused on four major process areas: gasification, zinc ferrite desulfurization, gas turbine, and SCR. Uncertainties in additional cost model parameters also were characterized, including direct and indirect capital costs, operating and maintenance costs, financial assumptions, and unit costs of consumables, byproducts, and wastes. Through an interactive screening process, the initial set of approximately 50 uncertain variables was narrowed to a set of 20 which most significantly affected uncertainty in plant efficiency, emissions, capital cost, and total levelized cost. These input uncertainty assumptions are given in Table 1. A sample size of 25 was used to illustrate the new capabilities. Figures 9 to 11 show the results of different stochastic optimization and stochastic programming problems applied to the IGCC flowsheet.

Figure 9 shows results of a stochastic optimization problem in which the expected cost of electricity (COE) is minimized for different levels of NO_x control. As the expected value of NO_x emissions is decreased, the cost of the optimal design increases, as does the expected value of NO_x removal efficiency in the SCR unit. As seen in Figure 9, the optimal design reduces the expected COE by 0.5 mills/kWh relative to the base case design achieving 0.44 lbs $NO_x/10^6$ Btu. For the 650 MW plant modeled in this example, this is equivalent to a total savings of approximately $2 million per year in plant costs resulting from the selection of optimal design parameters in the zinc ferrite and SCR units. Figure 9 also shows that the expected cost of the optimal design increases by 1.1 mills/kWh as NO_x is lowered from 0.6 to 0.2 lbs/10^6 Btu. Over this range, the optimal SCR removal efficiency increases from 73% to 90% (the maximum value established by the performance model). This limits the lowest achievable NO_x emissions to 0.22 lbs/10^6 Btu (expected value).

Table 1: Summary of Deterministic and Uncertainty Assumptions for the Illustrative Case Study.

DESCRIPTION AND UNITS (a)	DET VAL (b)	DISTRIBUTIONS AND THEIR PARAMETERS (c)			
		Type	Min	Max	Mode or Prob.
Gasifier Fines Carryover, wt-% of Coal Feed	5.0	F	0.0	1.0	5%
			1.0	3.5	20%
			3.5	5.0	25%
			5.0	8.0	25%
			8.0	15.0	15%
			15.0	20.0	5%
			20.0	30.0	5%
Fines Capture in Recycle Cyclone, wt-% of Fines Carryover	95	F	50	90	25%
			90	95	25%
			95	97	25%
			97	98	25%
Carbon Retention in the Bottom Ash, wt-%	2.5	T	0.75	10.0	2.5
Gasifier Coal Throughout, lb DAF coal/(h-ft2)	305	T	1.52	381	305
Gasifier NH3 Yield, % of coal-N converted	0.9	T	0.5	1.0	0.9
GAsifier Air/Coal Ratio, lb air/lb DAF coal	3.1	T	2.7	3.4	3.1
Steam/Coal Ratio, lb steam/lb DAF coal					
air/coal = 2.7	0.81	U	0.54	1.08	
air/coal = 3.1	1.55	U	1.24	1.86	
air/coal = 3.4	2.38	U	2.04	2.72	
Zinc Ferrite Sorbent Sulfur Loading, wt-% sulfur in sorbent	17.0	N	2.16	31.84	17.0
Zinc Ferrite Sorbent Attrition Rate, wt-% sorbent loss per absorption cycle	1.0	F	0.17	0.34	5%
			0.34	0.50	20%
			0.50	1.10	25%
			1.10	1.50	25%
			1.50	5.00	20%
			5.00	25.00	5%
Fuel NOx, % conversion of NH3 to NOx	90	T	50	100	90
Gasifier Direct Cost Uncertainty, % of estimated direct capital cost	20	U	10	30	
Sulfuric Acid Direct Cost Uncertainty, % of estimated direct capital cost	10	U	0	20	
Gas Turbine Direct Cost Uncertainty, % of estimated direct capital cost	25	U	0	50	
SCR Unit Catalyst Cost, $/ft3	840	U	250	840	
Standard Error of HRSG Direct Cost Model, $ Million	0	N	-17.3	17.3	
Maiintenance Cost Factor, Gasification, % of process area total cost	3	T	2	12	3
Maintenance Cost Factor, Combined Cycle, % of process area total cost	2	T	1.5	6	2
Unit Cost of Zic Ferrite Sorbent, $/lb	3.00	T	0.75	5.00	3.00
Indirect Construction Cost Factor, %	20	T	15	25	20
Project Contingency Factor, %	17.5	U	10	25	

(a) DAF = dry, ash free; SCR = selective catalytic reduction; HRSG = heat recovery steam generator

(b) DET. VAL. = deterministic (point-estimate) value.

(c) The first column indicates the type of distribution, where F = fractile, T = triangular, N = normal, and U = uniform. The remaining columns provide the parameters of the distribution.

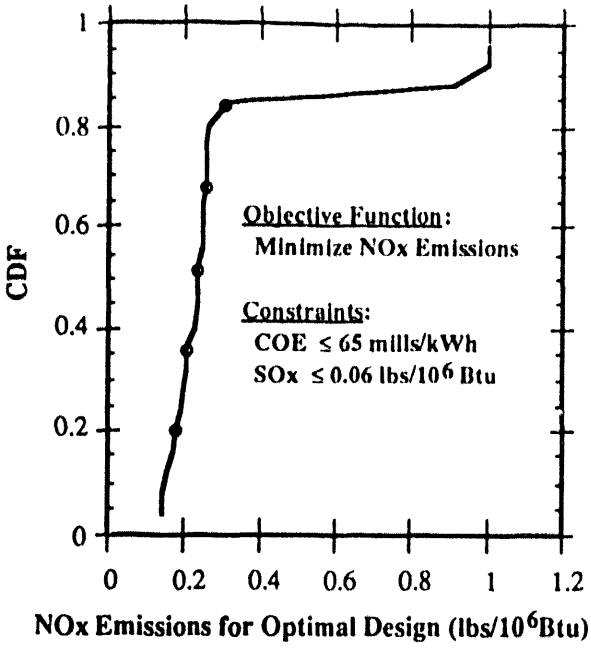

Figure 11: Effect of Uncertainties on Minimum NOx Emissions.

Figure 10 next shows the effect of uncertainties on the cost of an optimal design for the case of NO_x emissions constrained to 0.5 lbs/10^6 Btu or less, and SO_2 emissions to 0.06 lbs/10^6 Btu or less. The cost of electricity for the optimal design configuration varies by more than a factor of two due to the performance and cost uncertainties shown earlier in Table 1. An 80% confidence interval gives expected costs between 52.5 and 70.0 mills/kWh. Also there is a 5% probability of no feasible design able to meet the emission constraints with the assumed uncertainties.

Finally, Figure 11 shows an example in which NO_x emissions are minimized subject to a constraint on the maximum cost of electricity (in this case, 65 mills/kWh), representing an assumed upper bound on economic risk. The stochastic programming results for this case show a 50% probability of optimal designs achieving between 0.2 and 0.3 pounds $NO_x/10^6$ Btu. The mean value of the probabilistic results show a minimum NO_x emission rate of 0.32 lbs/10^6 Btu for this case. However, Figure 11 also shows a 15% chance of exceeding 0.6 lbs/10^6 Btu, which is the Federal New Source Performance Standard (NSPS) for coal-fired power plants. Thus, reducing process uncertainties or modifying process configuration to reduce the level of risk may be warranted.

These results are intended only to be illustrative of the new modeling capabilities now possible with stochastic optimization and stochastic programming. Additional case studies for other advanced power systems, including pressurized fluid bed combustion (PFBC) and externally fired combined cycle (EFCC) systems currently are in progress, and will be reported at a future date. In conjunction with these efforts, on-going work also is developing new or improved cost and performance models for selected process components and systems for IGCC, PFBC and EFCC designs.

5 Conclusions

This paper has presented new systems analysis tools and methodologies that can substantially improve the design and analysis of advanced coal-based energy systems of interest to DOE/METC. By combining existing process simulators with the mathematical methodologies presented here (i.e., probabilistic modeling, optimization, and MINLP synthesis) researchers and research managers now can tackle a wide range of system performance and cost analysis not heretofore possible. This new toolbox can be used in conjunction with new or existing process performance and cost models to insure that process design issues are more fully and rigorously considered in all phases of activity. These modeling tools also can be extended to a host of other technology applications where process design, cost minimization, risk analysis, environmental compliance, and R&D prioritization remain important issue.

6 References

Biegler L. T. (1983) Simultaneous Modular Simulation and Optimization, Proceeding of Second International Conference on Foundations of Computer Aided Process Design.

Biegler L.T. and J.E. Cuthrell (1985) Improved Infeasible Path Optimization for Sequential Modular Simulators, Part II, Computers and Chemical Engineering, 9:257-271.

Diwekar U. M., H. C. Frey, and E. S. Rubin (1992), Synthesizing optimal flowsheets: applications to IGCC system environmental control, *I&EC Res.*, **31**, 1927.

Diwekar U. M., I. E. Grossmann, and E. S. Rubin (1991), An MINLP process synthesizer for a sequential modular simulator, *I&EC Res.*, **31**, 313.

Diwekar U. M. and E. S. Rubin (1991), Stochastic Modeling of Chemical Processes, *Comput. chem. Engng.*, **15**, 105.

Diwekar U. M. and E. S. Rubin (1993), An Efficient Handling of the Implicit Constraints Problem in the ASPEN MINLP Process Synthesizer, *I&EC Res*, **32**, 2006.

Diwekar U. M. and E. S. Rubin (1994), Parameter Design Method using Stochastic Optimization with ASPEN, *I&EC Res*, **33**, 292.

Frey H. C. (1993), Performance Models of Selective Catalytic Reduction NO_x Control Systems, Quarterly report from Carnegie Mellon University to U.S. Department of Energy, Pittsburgh, PA 15213.

Frey H. C. and E. S. Rubin (1992a), Evaluation of Advanced Coal Gasification Combined-Cycle Systems under Uncertainty, *I&EC Res*, **31**, 1299.

Frey H. C. and E. S. Rubin (1992b), Integration of Coal Utilization and Environmental Control in Integrated Gasification Combined Cycle System, *Env. Sci. Tech.*, **26**, 1982.

Frey H. C., E. S. Rubin, and U. M. Diwekar (1994), Process Modeling of Advanced Technologies Under Uncertainty, *Energy*, **19 (4)**, 449.

Gill P.E., W. Murray, and M. H. Wright (1981), Practical Optimization, Academic Press, London.

Holt N. A., E. Clark, and A. Cohn (1989), NO_x Control in Coal Gasification Combined Cycle Systems, Symposium on Stationary Combustion Nitrogen Oxide Control Volume 1, GS-6453, Electric Power Research Institute, Palo Alto, CA, July 1989, 5A-17.

Kravanja Z. and I. E. Grossmann (1990), PROSYN-An MINLP synthesizer, *Comput. chem. Engng.*, **14**, 1363.

Lang Y. D. and L. T. Biegler (1987), A Unified Algorithm for Flowsheet Optimization, *Comput. chem. Engng.*, **11**, 143.

Marsten R. (1986), User's Manual for ZOOM/XMP, The Department of Management Information Systems, University of Arizona: Tucson.

Massachusetts Institute of Technology, ASPEN User's Manual, Vol. 1. Reports DOE/MC/16481-1203. NTIS/DE82020196 (1982).

P24 Development of a Radio Frequency Surface Contour Mapping System

CONTRACT INFORMATION

Contract Number W-7405-Eng-82 (Ames)
93MC30134.000 (METC)

Contractor Ames Laboratory
Iowa State University
Ames, IA 50011
(515) 294-3758

Contractor Project Manager William H. Buttermore

Principal Investigators Robert J. Weber
Warren E. Straszheim

METC Project Manager Margaret A. Kotzalas

Period of Performance January 1, 1993 to continuing

Schedule and Milestones

FY94 Program Schedule

	O	N	D	J	F	M	A	M	J	J	A	S
Design of a proof-of-concept RF-SCMS	———	———	———	———	———	———						
Fabrication of a proof-of-concept RF-SCMS and laboratory testing.							———	———	———			
Design of a phased array RF-SCMS system										———	———	———

OBJECTIVES

A radio-frequency based system is being developed for imaging the top surface of the contents of vessels used in coal processes including lockhoppers, gasifiers, and mixing chambers. The system will be designed to image a minimum of 25 pixels with a depth resolution

of ±1 inch over ranges of 4 to 30 feet. The system must tolerate harsh environments as found in coal gasifiers with temperatures up to 1800 F and pressures up to 600 psig). The system will provide both a visual readout of the contour of the upper surface of a vessel's contents via a computer monitor and a data interface to the process control system.

BACKGROUND INFORMATION

The capability to continuously monitor the contents of a vessel is important to many aspects of coal utilization. Vessels of concern include gasifiers, storage silos, lockhoppers, etc. Surface monitoring and mapping can be important since interruptions in the designed flow of materials can severely disrupt or shut down coal processes.

METC developed an acoustic-based surface contour monitoring system which used an array of transmitters and receivers to monitor multiple locations within a vessel. However, acoustic-based systems can be affected by the extreme conditions within many of these vessels, while RF-based systems are more immune to such interference.

PROJECT DESCRIPTION

Design of a radio frequency surface contour mapping system is building upon a similar surface contour mapping device developed by Morgantown Energy Technology Center (METC) which used acoustic signals. The first stages of work include assessment of the conceptual design for the radio frequency-based surface contour mapping system (RF-SCMS) developed at METC and development of a design for an RF-SCMS system. This will be followed by fabrication and laboratory testing of a proof-of-concept system utilizing mechanical scanning of a single-channel RF system. Following testing of the proof-of-concept system, a design will be developed for a multiple channel, phased array system. Following initial tests of that system in the laboratory, the system will be hardened as necessary to withstand harsh environments and then subjected to field tests under actual process conditions.

RESULTS

Work to date has focused on review of the METC design and engineering analysis of the radar-based system. Extensive simulations have been performed to determine the lateral and depth resolution of the system. Initial results indicate that a 4.3 GHz system using a 9-antenna array should be able to achieve a depth resolution of 1 inch and a beam size of 25 inches at 20 feet which could be used to image about 10 pixels within a 6-foot vessel. Work is also proceeding on development of delay-and-sum algorithms for steering the beam about the vessel.

Figures 1 and 2 below show the actual and reconstructed surface for one test arrangement. In this case, a 9-element antenna array was positioned 10 m (32.8 ft)above the floor of a vessel 2 m (6.6 ft) in diamter. The test surface was at a height of 3.0 m (9.8 ft) with a ridge of 3.5 m (11.5 ft) across the center of the vessel. The reconstructed surface clearly shows the ridge across the center of the vessel. Additional tests are in progress to determine the best possible resolution for a given number of antennas in the array.

A demonstration system built around a 4.3 GHz radar transmitter/receiver is being assembled for the proof-of-concept system, and laboratory facilities have been prepared. All equipment, including a data acquistion system, have been acquired and are being installed.

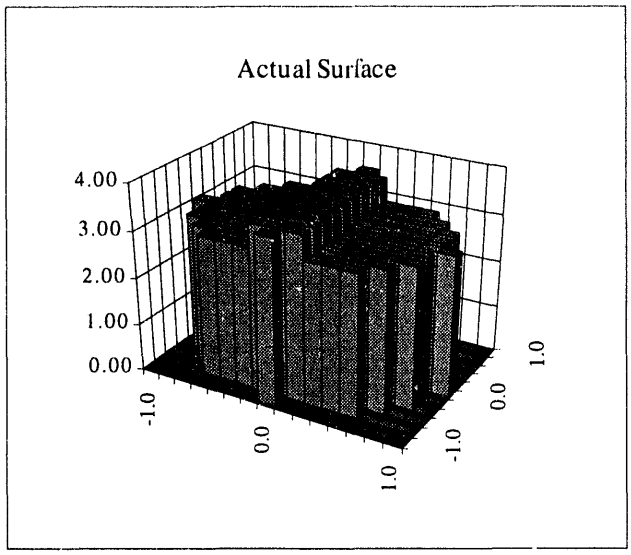

Figure 1. Original Test Surface

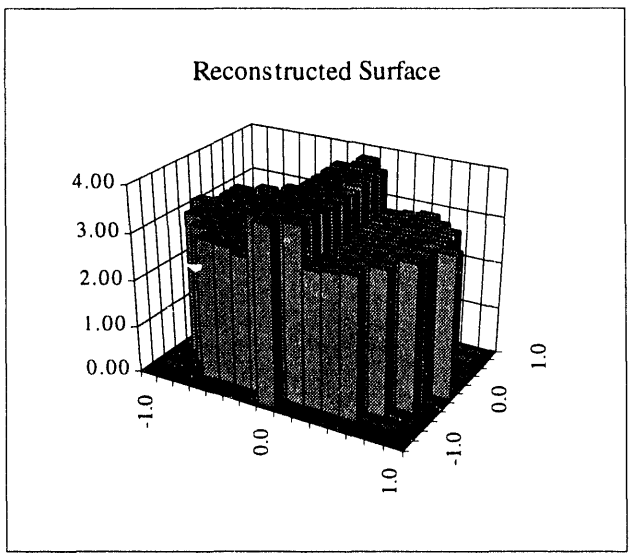

Figure 2. Surface Reconstructed from Calculated Data

Tests of the system will verify the computer simulations and data processing algorithms, and aid in the design of the actual SCMS which will utilize multiple antennas. Issues to be addressed include the size and placement of the antenna array and the operating frequency of the system. A higher frequency system operating at 35 GHz would provide improved resolution and will likely be adopted for the final design.

FUTURE WORK

In future work, the full SCMS will be constructed using multiple antennas and using electronic switching. The system will be hardened for testing on actual, operating structures and will be modified as needed to achieve the necessary performance.